POLITECNICO DI TORINO

DIMEAS - Department of Mechanical and Aerospace Engineering

College of Mechanical, Aerospace, Automotive and Production Engineering

"Master of Science in Mechanical Engineering"

PROCESS MODELING OF THERMOPLASTIC COMPOSITES FOR WIND TURBINE BLADE

PoliTo Supervisor: Dr. Maria Pia Cavatorta (Politecnico di Torino)

UML Supervisor: Dr. Marianna Maiaru (University of Massachusetts Lowell)

Student: Muhammad Fahad Mohsin

APRIL 2021

Thesis submitted in compliance with the requirements for the Master of Science degree

PREFACE

This written master's thesis is based on computational mechanics' study perform remotely at University Massachusetts Lowell for thermoplastic composites. This master thesis is weighted with 18 credits in the ECT system and has completed under the "Tesi su Proposta" Program from Politecnico Di Torino, Italy. Under this program, Dr. Maria Pia Cavatorta from Politecnico Di Torino has supervised as the internal supervisor while Dr. Marianna Maiaru from University of Massachusetts Lowell has supervised as an external supervisor.

It has been an honor to work under remarkable professors and scientists in their fields and have written this thesis in their supervision. Besides the principal supervisors, I am also very thankful to my colleagues of $\boldsymbol{i}\mathbf{Comp}^{\mathbf{2}}$ group at University of Massachusetts Lowell specially Sagar Shah (Ph.D. Student) and Michael Olaya (Ph.D. student) for helping and supporting me throughout my subroutine analysis of thermoplastic composites on Abaqus software. Their feedback, support, and knowledge have been very beneficial. I am grateful to Dr. Greg Odegard and his team, in particular Swapnil Bamane (Ph.D. student) at Michigan Technological University for their collaboration related to my thesis work.

I want to express my most profound appreciation to both of my Internal and External Supervisors, for the time they dedicated to my work, for excellent assistance, for ideas on how to solve problems on the way, as well for their enthusiastic encouragement.

Finally, I would like to thank my family and friends, especially from Politecnico Di Torino, to provide extra confidence in me during this tenure.

ABSTRACT

This work proposes process modeling simulation for future manufacturing of wind turbine blades using fully recyclable thermoplastic composites. The formation of crosslinks in thermosets composites makes them non-eco-friendly and difficult to recycle, resulting in a massive amount of composite material to the waste stream. The use of thermoplastic resins versus their thermosetting counterparts can potentially introduce cost savings due to non-heated tooling, shorter manufacturing cycle times, and recovery of raw materials from the retired part.

Thermoplastic resin systems have long been discussed for use in large-scale composite parts but have yet to be exploited by the wind energy industry because of their manufacturability. A newly developed ELIUM thermoplastics by Arkema has been studied for its unique combination of mechanical properties and manufacturability. ELIUM is characterized by high impact resistance, post-thermoform ability, and it is fully recyclable. Additionally, ELIUM can be manufactured through infusion and in-situ polymerization, enabling mass production of large components. Specifically, ELIUM-150 is used in this work, which has a low viscosity and will be suitable for manufacturing wind blades through the infusion process. Process modeling is performed using Abaqus to predict the temperature evolution and Degree of Polymerization via user-written subroutines. A wind turbine blade geometry is modeled accounting for its various components, composite lay-ups, and manufacturing cycle. Additional modeling is proposed to analyze the spar-cap area of the blade. An optimization study is performed to determine a polymerization cycle that would guarantee the fastest possible time to homogenously polymerize the composite wind blade while maintaining a low exothermic heat of reaction during manufacturing.

Contents

Chapter#1

1 Introduction

Due to their high strength- to-weight ratio, fracture toughness and damage tolerance, Fibre reinforced thermoplastic composites (FRTPCs) are widely used in high-end aerospace and aircraft industries. As compared with their thermoset counterparts, the processing speed of thermoplastic composites is relatively fast. In general, a melt process is used to manufacture structural FRTPCs in which the thermoplastic resin is melted, formed and solidified. The significant drawbacks of this thermal processing are the high processing temperatures and pressures together with relatively high viscosity of the thermoplastic material which limit the manufacturing of FRTPC parts in size and thickness [1]. An alternative to melt processing of the FRTPCs is the in-situ polymerization of monomeric or oligomer thermoplastic materials. Some examples of reactive thermoplastic resins are the thermoplastic polyurethanes (TPUs), polyamides (PAs), poly ethyl eneteraphthalate (PET), poly- butyl eneteraphthalate (PBT) and Polycarbonate (PC) [1]. Another example is the recently developed Elium® acrylic resin which is composed of 2-Propenoic acid, 2-methyl-, methyl ester or methyl- methacrylate monomer (MMA) and acrylic copolymers in which MMA undergoes a free radical polymerization to its polymer PMMA. The advantage of commercially available Elium® is that the polymerization can take place at relatively low temperatures even at room temperature. In reactive processing of Elium® composites, the fiber reinforcements are first impregnated with the resin which is in a liquid state at room temperature with a relatively low viscosity. Afterwards, the in-situ polymerization takes place by mixing the MMA monomers with compatible initiator systems such as a peroxide and applying stimuli such as heat, microwave or ultraviolet. One of the major challenges in processing fiber reinforced Elium® composites is the presence of internal overheating due to the exothermic reaction of the radical polymerization which is also seen in thermoset resins during the curing or cross-linking of the molecular groups. This might result in boiling of the thermoplastic resin and hence voids in the composite part. In addition, the large temperature difference can take place in thick composite manufacturing, which results in unwanted residual stresses and shape distortions

as extensively investigated in thermoset composites [2–4]. Therefore, the polymerization reaction of Elium® composites has to be understood, described and predicted well in order to develop reliable FRTPCs by using the reactive manufacturing processes such as vacuum assisted resin transfer molding and pultrusion. The previous researches on Elium® resins and their composites are summarized in the following. Barbosa et al. [5] compared the behavior of Elium® 150 in mode II interlaminar fracture with the traditional epoxy matrix, and found that it can resist up to 40% more than epoxy matrix composites based on the end notched flexure tests. With the optimized welding parameters of a weld time of 1.5 s and a weld pressure of 3 bar, the maximum lap shear strength of the welded carbon/Elium® composite laminate was found to be 23.2% higher than the adhesively bonded Elium® laminates [6]. Bhudolia et al. [7] studied mode I interlaminar fracture toughness (ILFT) behavior of Elium® composites. The results showed that the ILFT properties of thin ply thermoplastic composites was found to be 30% higher than the thick ply thermoplastic composites. Zoller et al. [8] optimized the process temperature by analyzing the radical polymerization of the acrylic resin and compared the conversion degree of the resin with different types of initiators. Elium® composites exhibited lower damage and higher residual strain than the epoxy composite through the load-unload cycles as reported in [9]. The advantage of the Elium® resin composite system in the vibration damping was presented in [10] by vibration and dynamic mechanical analysis tests and its structural damping was found to be 27% higher than the epoxy composites. Boumbimba et al. [11] found that the addition of acrylic tri-- block copolymers led to an increase in impact resistance for test temperatures of 80 ◦C. This improvement was approximately 24% in terms of the penetration threshold. Kinvi-Dossou et al. [12] investigated the impact performances of Elium® composites and found that the delamination extension of acrylic composite was smaller than the one for epoxy composites. In addition, the moisture diffusion behavior of Elium® composites was investigated in [13]. The results indicated that the weight gain at the saturation of flax-acrylic composite was found to be lower than that of flax-epoxy composite. The characterization of Elium® 150 polymerization reaction was studied in [14] and it was shown that the polymerization was influenced both by the peroxide initiator and the temperature. An optimized thermal cycle for the polymerization of Elium®150 resin was proposed in Cadieu et al. [15] studied the loading rate effect on the mechanical properties of a glass/Elium® 150 laminated composites. The

results indicated that the loading rate had a significant influence on the macroscopic parameters of the behavior of the samples. Nash et al. [16] investigated the effect of environmental conditioning on the apparent interlaminar shear strength and dynamic mechanical properties of well-established marine resin systems- and Elium® -matrix composite materials. It was demonstrated that the infusible Elium® resin could be a candidate for the use in marine structures. Kazemi et al. [17] studied the mechanical properties of an ultra-high-molecular-weight polyethylene fabric/Elium® laminates and found that Elium® can be a competitive resin to replace the traditional resins for the fabrication of composite structures. An advanced cure monitoring system and a microwave system were developed and utilized to manufacture Elium® composites in [18]. The temperature evolution and resistance of Elium® composite were determined to obtain a better microwave heating by achieving a 25% increase in the speed of Elium® reaction. The chemical kinetics and rheology of a partially polymerized carbon/PMMA prepregs were investigated in [19] to develop materials processing guidelines for reactive thermoplastic prepregs.

Although Elium® thermoplastic resins and their composites were investigated by several researchers, to date there has been a limited focus on the exothermic reaction and resulting polymerization over- heating in literature. It was stated in [20] that the highly exothermic reaction during the manufacturing of thick Elium® composites (12 mm or greater) could cause the peak temperature being higher than the resin boiling temperature of 100 ◦C. This might cause an uncontrolled temperature distribution and growth as well as process instabilities and unwanted monomer loss due to the boiling of the resin.

1.1 Background

Fiber-reinforced polymer composites are a desirable class of structural engineering materials due to their high specific mechanical properties. They are increasingly used in the construction, automotive, aerospace, and energy sectors (Mazumdar et al., 2017). Electricity generated from wind turbines has grown consistently by approximately 7.3 GW of installed capacity every year for the last decade in the United States (American Wind Energy Association, 2017). Wind turbine blades are constructed with fiber reinforced polymer and balsa or foam core; landfilling turbine blades contributes a massive amount of composite material to the waste stream. One study estimates 9.6 metric tons of composite per megawatt

of installed capacity (Arias, 2016). Such waste of highly engineered material represents not only an environmental issue, but also a loss of potentially recoverable capital. Thermoplastic resins, which are inherently recyclable (Jacob, 2011), are potentially a better design choice due to increasing regulation of composite waste landfilling. The European Union Directive on Landfill Waste has enacted legislation that prohibits disposal of large composite parts such as wind turbine blades (1999/31/EC). It is prudent to anticipate the potential for similar legislation in the United States; therefore, it is a primary objective of the Institute of Advanced Composites Manufacturing Innovation to qualify composite technologies of which 80% of the constituent materials can be reused or recycled (IACMI, 2018).

Thermosetting resins such as epoxy, vinyl ester, and poly(urethane) dominate the composites market; the wind industry exclusively uses these resins for vacuum infusion of blades. However, there is an increasing trend toward using thermoplastic resins in long fiber composites outside of the wind industry and a growing interest for using these resins in blade fabrication (Yao et al., 2018). Presently, there are several options for wind turbine blades at the end of their service lives: direct deposit in a landfill, grind for use as aggregate in concrete, or incineration with energy recovery (Correia et al., 2011; Fox, 2016; Larsen, 2009; Papadakis et al., 2010; Ribeiro et al., 2015). Additionally, a recent study has shown that thermoset blades can be recycled via grinding to be used for construction materials (Mamanpush et al., 2018). That these recycling techniques are not commercially exploited on a large scale demonstrates the small margins on which they operate. Thermoplastics can potentially limit the extent of down-cycling that thermoset composites require. Still, the viability of composite recycling is heavily dependent upon reintroduction of recovered materials into the supply chain to displace virgin materials (Li et al., 2016; Witik et al., 2013).

The current investigation quantifies and demonstrates the methods by which the Elium thermoplastic resin system (Arkema, 2018) can facilitate recycling of large-scale composite parts by recovering and reusing material from a component of a wind turbine blade [21]. A portion of a spar cap, which acts as the end of the I- beam structure in the interior of the blade, was used for this study. Four recycling techniques are considered, including thermal decomposition of the polymer matrix, mechanical grinding, thermoforming, and dissolution.

The decomposition energy of a commercial epoxy and Elium are compared via simultaneous thermal analysis (STA), which combines thermo gravimetric analysis (TGA) and differential scanning calorimetry (DSC). The tensile properties of recycled thermoplastic regrind are compared to those of similar virgin material. Thermoforming is demonstrated on a thermoplastic spar cap, and test panels are thermoformed to make a prototypical skateboard. Energy requirements for dissolution of thermoplastic components and separation into their constituent materials are estimated. Further, the tensile mechanical properties of glass fibers recovered from the dissolution experiment are compared to those of virgin glass fibers. Dissolution of thermosets is not possible, and therefore only the thermoplastic system is investigated using this recycling technique. Finally, the technical results from the investigation of the dissolution technique are used in an economic analysis to assess the commercial viability of recycling.

1.2 Motivation

The main motivation to work on the process modelling of thermoplastic composites for wind turbine blades is replace thermoset composites which are currently being used widely in the manufacturing of wind blades. Following are the foremost reasons that are making this research activity more stimulating to replace thermoplastics and are explaining the major disadvantages for this type of polymeric substance;

- **Hazardous for environment**

  Thermoset composites are not environment friendly because they have a very long life span to naturally degrade which is around 500 years.
- **Cross-linked molecular structure**

  Thermosets are the type of polymeric compound which cannot be remold or reshape because of its molecular structure which has cross-linked between each other and very difficult to break in case of recycling.
- **Wastage of highly engineered material**

  Since thermoset materials do not melt again once cured, to mechanically recycle thermoset matrix composites it is necessary to size reduce them. Steps required to transform recyclate into reduce size are highly energy intensive.

- **Contribution to landfills**

  As the wind turbine blade are big in size, they are difficult to dispose off in the landfills. Even the landfill areas are sufficient enough to contain all the waste of thermoset composites once the production will increase for the manufacturing of wind blades because the energy sector is currently shifting towards the sustainable energy options and wind energy is also one of the best alternate source of energy.

1.3 Aims and Objectives

The main objective of this study is to work on an alternative material for the manufacturing wind turbine blade. Thermoplastic resin systems have long been discussed for use in large-scale composite parts but have yet to be exploited by the energy industry. The use of these resins versus their thermosetting counterparts can potentially introduce cost savings due to non-heated tooling, shorter manufacturing cycle times, and recovery of raw materials from the retired part. Because composite parts have high embedded energy, recovery of their constituent materials can provide substantial economic benefit. This study determines the feasibility of recycling composite wind turbine blade components that are fabricated with glass fiber reinforced Elium® thermoplastic resin. Several experiments are conducted to tabulate important material properties that are relevant to recycling, including thermal degradation, grinding, and dissolution of the polymer matrix to recover the constituent materials. Dissolution, which is a process unique to thermoplastic matrices, allows recovery of both the polymer matrix and full-length glass fibers, which maintain their stiffness (190 N/(mm g)) and strength (160 N/g) through the recovery process. Injection molded regrind material is stiffer (12 GPa compared to 10 GPa) and stronger (150 MPa compared to 84 MPa) than virgin material that had shorter fibers. An economic analysis of the technical data shows that recycling thermoplastic glass fiber composites via dissolution into their constituent parts is commercially feasible under certain conditions. This analysis concludes that 50% of the glass fiber must be recovered and resold for a price of $0.28/kg. Additionally, 90% of the resin must be recovered and resold at a price of $2.50/kg [21].

Therefore, this research activity is used to critically assess the exothermic reaction and overheating during manufacturing of wind turbine blade with Elium® based thermoplastic composites. The polymerization kinetics of the Elium® resin is investigated by performing

isothermal and dynamic differential scanning calorimetry (DSC) tests [22]. To this end, a temperature dependent kinetics model is developed based on the data fitting analysis. The obtained kinetics model and the total heat of polymerization reaction are used in the transient thermo-chemical model to predict the temperature and degree of polymerization (DoP) evolutions during the manufacturing process.

In order to study the newly developed Elium® thermoplastic resin by Arkema, we have used a multiscale modeling approach to scale down the modeling of a polymeric substance. It will allow us to integrate physics-based knowledge to bridge the scales and efficiently pass information across temporal and spatial scales.

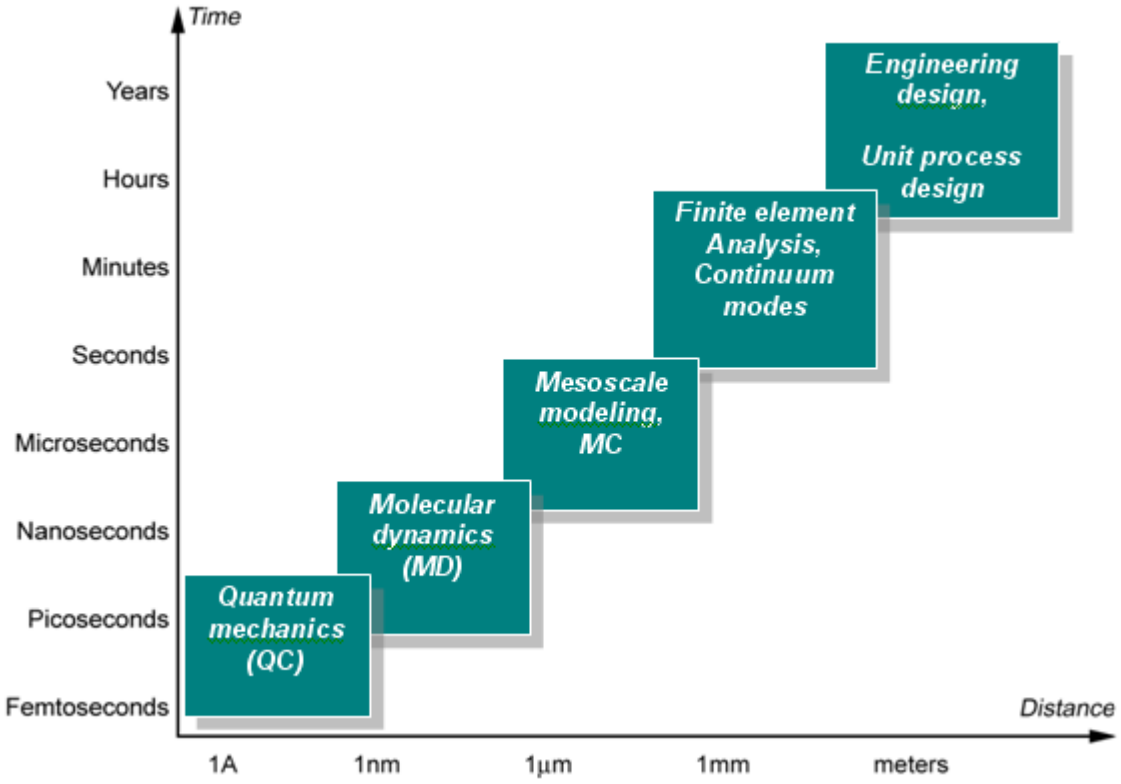

Fig.1.1: An illustration for multiscale modeling approach

For multiscale modeling approach, the research work has been classified in two teams based on the molecular dynamics simulation and process modeling of Elium resin to predict the response of the material. Molecular dynamics work has been dedicated to the team in Michigan Technological University under the supervision of Dr. Greg Odegard. While the

process modeling work has been assigned to the team in University of Massachusetts Lowell (***i*Comp^2** group) under the supervision of Dr. Marianna Maiaru. As a part of ***i*Comp^2** group, my research work is also specifically related process modeling of thermoplastics composites for the manufacturing of wind turbine blade.

1.4 Novelty

In this thesis, Numerical simulations have performed to develop a model for wind turbine blade that can be manufacture through thermoplastic material. For thermoplastic material, it is described about recently developed chemical compound named as Elium by Arkema company. Elium® resins can be molded by infusion at room temperature to make large and stiff structural parts, with excellent toughness. Low viscosity and long gel time ensure excellent fiber impregnation to reach optimum mechanical properties. Carbon fiber and glass fiber can be used. Structural bonding is possible with AEC Polymers adhesives.

1.5 Chapters Distribution

This thesis is divided into six main sections (Chapters).

Chapter 1 (Introduction) is about relevant background theory, which provides an overview of this study, aims and objectives, and novel approaches for the process modelling of thermoplastic composites.

Chapter 2 (Literature review) contains the theory related to the thermoplastics, its classification, different types of equipment and material used for its application, and the effects of different parameters on polymerization process.

Chapter 3 (Manufacturing of Wind Blade) describes the manufacturing processes and details related to the components being used to build up the complete structure of blade.

Chapter 4 (Process Modelling of Wind Blades) explains the polymerization kinetic model along with description of all boundary conditions applied in sub routine analysis.

Chapter 5 (Results and discussions) In this section, the results from the study have discussed the graphs and images obtained from Abaqus Software.

Chapter 6 (Conclusion and recommendations) concludes the aim of the experimental study and the overall summary of the research along with the future directions to extend the process modelling of thermoplastics composites for wind turbine blade.

Chapter #2

2 Thermoplastics Literature Review

Thermoplastic polymers differ from their thermoset counterpart primarily by their melt temperature being lower than their decomposition temperature, while thermoset polymers have melting temperatures higher than their decomposition temperature, meaning that they cannot be reshaped upon melting. In molecular terms, this characteristic can be correlated to molecular weight, since an increase in molecular weight increases the melting temperature. Thermoset have very high molecular weights because of the cross-links between their polymer chains, while thermoplastics have lower molecular weight since they are generally not cross-linked.

The fundamental difference in physical properties between thermosets and thermoplastics has governed the development of their respective manufacturing techniques over the years with thermoplastic usually being melt processed while thermosets are exclusively reactively processed.

2.1 Classification of Thermoplastics:

Most thermoplastics have a high molecular weight. The polymer chains associate by intermolecular forces, which weaken rapidly with increased temperature, yielding a viscous liquid. In this state, thermoplastics may be reshaped and are typically used to produce parts by various polymer processing techniques such as injection molding, compression molding, calendaring, and extrusion. Thermoplastics differ from thermosetting polymers (or "thermosets"), which form irreversible chemical bonds during the curing process. Thermosets do not melt when heated, but typically decompose and do not reform upon cooling. Based on the polymerization reaction, thermoplastics has been divided in 2 following types;

2.1.1 Vinyl polymerization

Vinyl polymers are polymers made from vinyl monomers: small molecules containing carbon-carbon double bonds During polymerization the double bonds are broken into single bonds, resulting in two free electrons Then these monomer units will form a long chain of many thousands of carbon atoms containing only single bonds between atoms. Examples are Polyethylene, Polypropylene, Polystyrene, Poly methyl metacrylate (Elium) etc. [23]

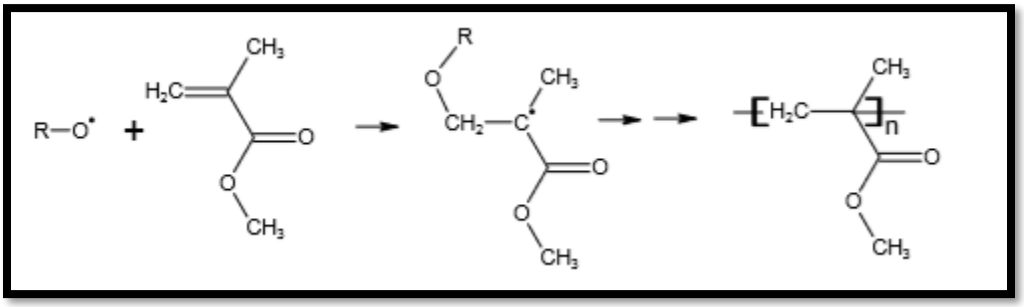

Fig. 2.1: Formation of Vinyl Polymers from Monomers

2.1.2 Ring-opening polymerization

Ring-opening polymerization (ROP) is based on a polymerization mechanism in which ring-shaped molecules (cycles) are opened into linear monomers or oligomers and subsequently connected into high molecular weight polymers without generating byproducts. The role of the initiator is to provide the polymeric chain with the necessary electrical charge for chain - growth in its anionic form (C6 H10 O N). The activator consists of derivated species from caprolactam, in which a carbamoyl group has been attached to its nitrogen atom. Examples are Polyethers, Polyamides etc. [23]

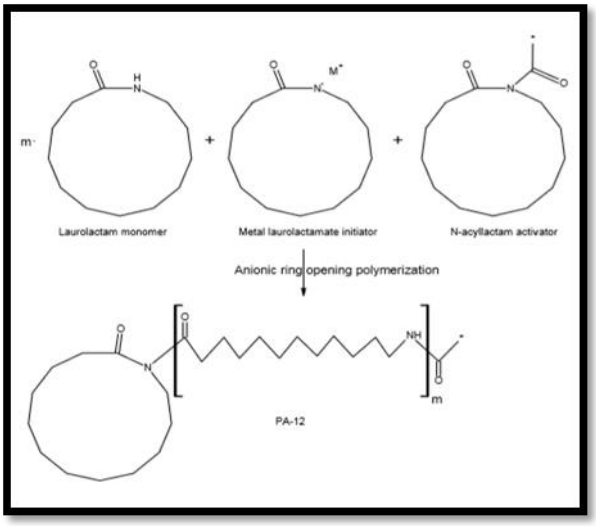

Fig. 2.2: Formation of Ring Shaped Polymers from linear monomers

2.2 Elium Thermoplastics:

FRPC laminates with traditional thermoplastic resins, namely PEEK, Cyclic Butylene Terephthalate (CBT), Polyurethanes (PU), to name but a few, are already well documented in the literature [24-27]. These resins are in film or pellet forms, which require high processing temperature and costly equipment [28]. As a result, compared to thermoset resins, they are rarely used [29-31]. Essentially, a room temperature curing thermoplastic resin is needed, which not only does not compromise the mechanical properties of composites, but also can be processed using liquid processing techniques like Vacuum Assisted Resin Infusion (VARI) and Resin Transfer Molding (RTM). The ELIUM® 150 is a low viscosity liquid, thermoplastic resin for infusion and RTM processes. Through the use of the same low pressure processes and equipment used today to produce thermoset composite parts, these formulations lead to the production of thermoplastic composites reinforced by continuous glass, carbon or natural fibers. The resulting thermoplastic composite parts show mechanical properties similar to those of parts made of epoxy resins while presenting the major advantages of being post thermoform able and recyclable and of offering new possibilities for composite/composite or composite/metal assemblies. The Elium® resin is a very promising resin for the production of recyclable advanced thermoplastic composites that can be used in a wide range of applications.

2.2.1 Typical Curing Characteristics

The ELIUM® resins are 2K based formulations that undergo radical polymerization to produce thermoplastic composite matrices. The polymerization is initiated by Peroxide compounds (Luperox®). Typical open time and peak time with 3% Luperox® EZ-FLO are: [32]

Reactivity(2) (200 grams)	Infusion open time	Injection open time	Peak time
15 °C	30 min.	35 min.	50 min.
20 °C	25 min.	30 min.	40 min.
25 °C	20 min.	25 min.	33 min.

Table. 2.1: Curing characteristics of Elium-150

The demolding can take place 5-10 minutes after reaching the peak exotherm. Open time is the amount of time during which the viscosity of the resin is low enough to inject the resin. Temperature and peroxide ratio will affect the open and peak times. The recommended peroxide ratio is from 1,5% (slow reactivity) to 3% (higher reactivity). Out of this range the resin will not polymerize properly. Room temperature polymerization leads to high conversion rate, so post-curing is generally not needed. If maximum mechanical properties are desired, post-curing at 80 °C for 4 hours is beneficial. Vinyl ester or epoxy molds with a glass transition of 100-120 °C are recommended.

2.2.2 Curing Time

Samples of Methyl Methacrylate (MMA) monomer immersed in constant T bath with J-Type thermocouples. Traditional thermoplastic resins, namely PEEK, Cyclic Butylene Terephthalate (CBT), Polyurethanes (PU), to name but a few, are already well documented in the literature. These resins are in film or pellet forms, which require high processing temperature and costly equipment.

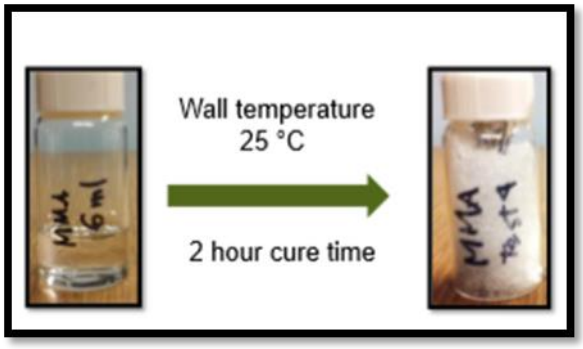

Fig. 2.3: Polymerization of Methyl Methacrylate (MMA) monomer at room temperature

As a result, compared to thermoset resins, they are rarely used. Essentially, a room temperature curing thermoplastic resin is needed, which not only does not compromise the mechanical properties of composites, Initiator is analogous to hardener / curative in epoxy systems. Less initiator means slower reaction and lower peak temperatures due to increased time for heat transfer. [33]

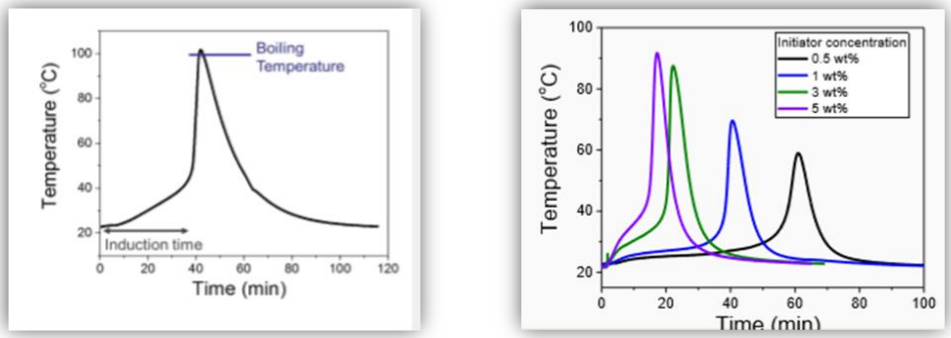

(a) (b)

Fig. 2.4: (a) Polymerization Cycle of Methyl Methacrylate (MMA) monomer (b) Influence of initiator on Polymerization Cycle of MMA

2.2.3 Effects of Flow Mesh Length

The carbon non crimp fiber (NCF) was first infused with full flow mesh (same as the size of the panel). However, the full flow mesh accelerated the flow in the longitudinal direction, the panel was not fully infused in the thickness direction, and a massive dry spot with entrapped air was noticed. Then, the infusion was carried without the flow mesh as shown in Figure to reduce the longitudinal resin flowrate. However, this attempt was not

successful. The infusion was too slow and resin reached its gel time before the infusion was complete.

		Flow Mesh Length (Per Cent of Total Laminate Length)					
		0%	50%	60%	70%	80%	100%
Observations on preform filling at 400 mbar infusion	Top surface of laminate	Cannot fully infuse (Figure 7a)	Small dry spot	Smaller dry spot	Small dry spot	No dry spot (Figure 7b)	No dry spot (Figure 7c)
	Bottom surfce of laminate	Cannot fully infuse (Figure 7a)	Massive dry spot	Massive dry spot	Small dry spot	Very small dry spot (Figure 7b)	Massive entrapped air (Figure 7c)
Quality		Not acceptable	Not acceptable	Not acceptable	Not acceptable	Acceptable	Not acceptable

Table. 2.2: Characterizing the quality of the laminate with Flow mesh length

Further, the panel was infused with reduced flow mesh length and resulted in much improved impregnation with only a small dry spot as shown in Figure. The flow mesh length (per cent of the total laminate length) was varied from 50% to 80% to achieve the right balance between the preform filling and the impregnation time [34]. Preform was better filled with reduced flow mesh lengths as compared to one with no and full flow mesh length.

2.2.4 Effects of Multi Vacuum Levels

Even though the thickness infusion was found to be significantly improved by reducing the flow mesh length, it was necessary to optimize the vacuum level and corresponding flow speed which has a detrimental effect on manufacturing of NCF laminates with low void content. Infusion of NCFs with both the matrices was carried out with one-, two-, and three-stage vacuum levels. The details of the vacuum levels used in single and multi-stage phases of infusion process. Single stage infusion was carried out at similar infusion and consolidation vacuum levels. Two-stage infusion was used where first the resin was infused at low vacuum levels for balancing the impregnation in the longitudinal and transverse direction.

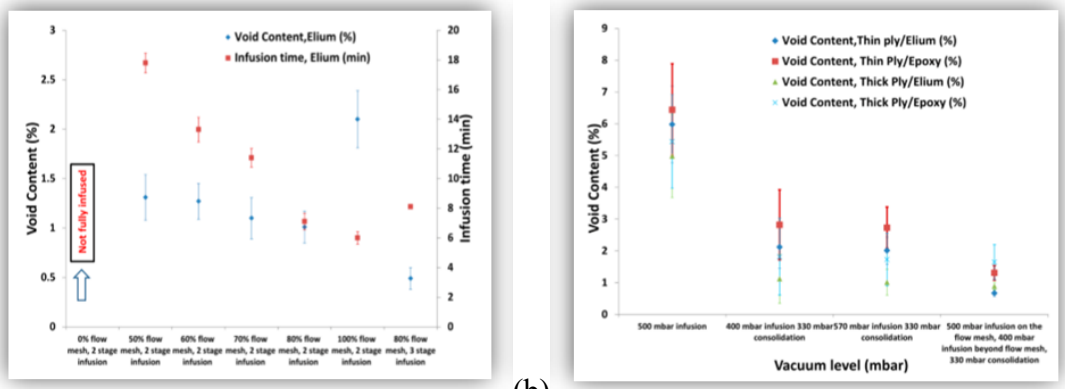

(a) (b)

Fig. 2.5: (a) Characterizing the Void content with Multi Vacuum Level and Infusion Time (b) Comparison of Void content between Elium and Epoxy resin

Once the infusion was completed, the consolidation was carried out at higher vacuum level. In the case of three-stage vacuum level, the preform was infused with reduced flow mesh and with three different vacuum levels (lower vacuum during infusion on the flow mesh, low vacuum level beyond the flow mesh till end of infusion and high vacuum level for consolidation) [34]. A lower vacuum level was used for infusion at the start to prevent the resin from boiling and to ensure a slow infusion for good fiber impregnation. Once the infusion was complete, the vacuum level was increased to ensure better consolidation and increased Vf.

2.2.5 Effects of Phase change materials

Phase Change Materials (PCMs) are substances which absorb or release large amounts of so-called “latent” heat when they go through a change in their physical state, i.e., from solid to liquid. With the thermal scanning, it can be seen that without PCM there is a Slow motion during the curing reaction the resin is transferred through the bag into the laminate, distributed by a channel or lining/mesh. Single stage infusion was carried out at similar infusion and consolidation vacuum levels [33].

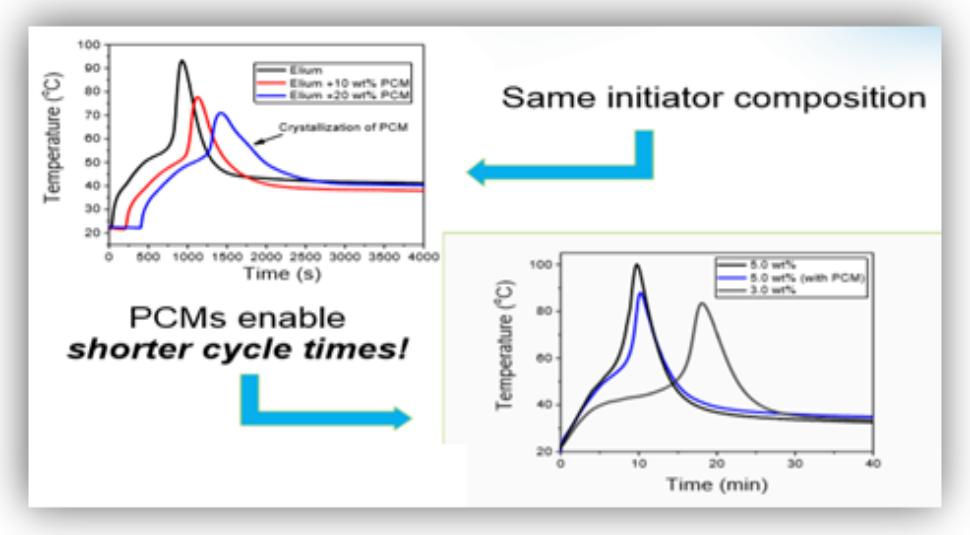

Fig. 2.6: Characterizing the change in Polymerization cycle due to the usage of Phase change material

Two-stage infusion was used where first the resin was infused at low vacuum levels for balancing the impregnation in the longitudinal and transverse direction. Once the infusion was completed, the consolidation was carried out at higher vacuum level.

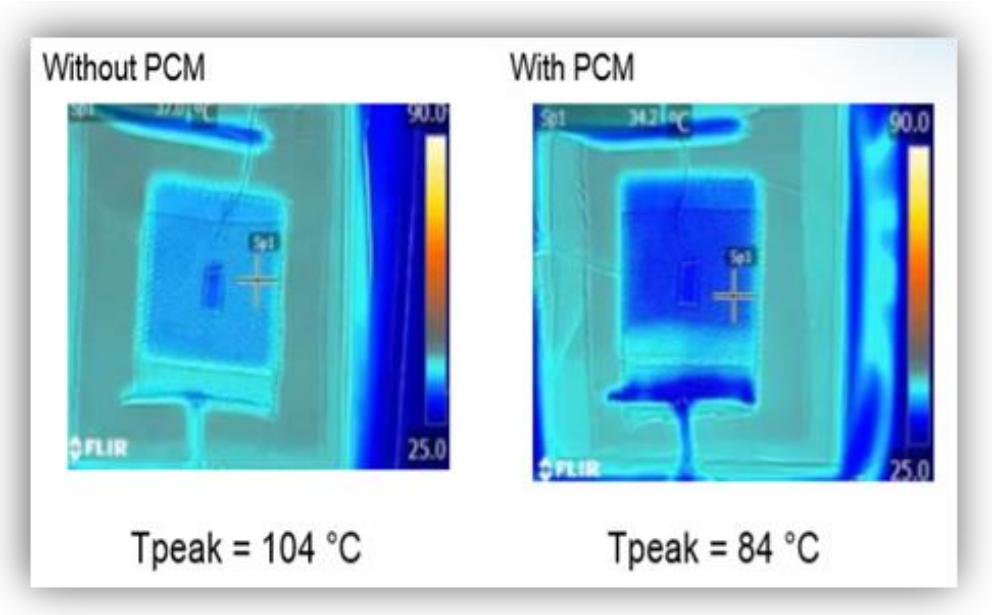

Fig. 2.7: Characterizing the exotherm peak temperature during Polymerization cycle due to the usage of Phase change material

2.2.6 Rheology and shrinkage data for simulation

Measure the viscosity as a function of time at a constant shear rate of 100 1/s with the gap fixed at 1 mm. Such a viscosity correlation is particularly useful – because the intrinsic viscosity is a function of molecular weight, the concentration needed to obtain a given viscosity for any given average molecular weight can be calculated.

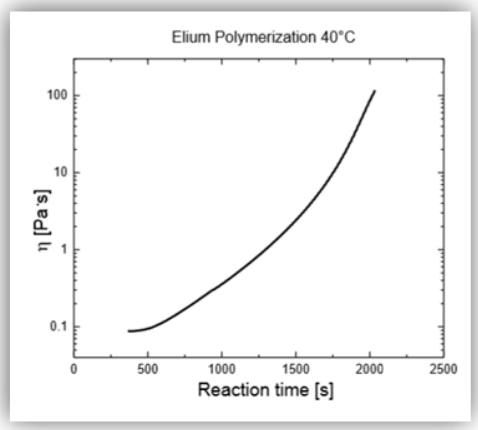

Fig. 2.8: Change in viscosity of Elium resin during the polymerization cycle

This viscosity correlation also provides a link to the kinetic models that can predict conversion. Storage modulus (E') is a measure of elastic response of a material. It measures the stored energy. When the torque on the geometry reaches a cutoff value, switch to an oscillatory measurement at 3.33 rad/s and allow the gap to change to produce an applied normal force of 0.5 N. [33]

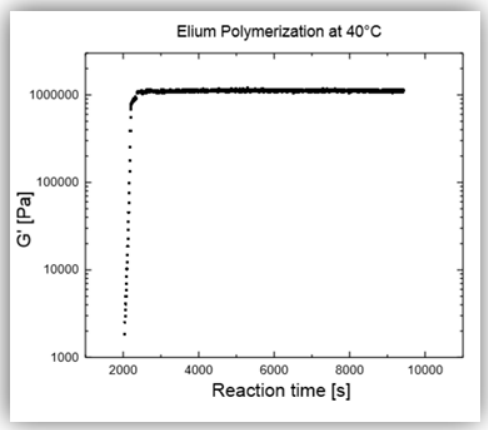

Fig. 2.9: Change in Storage modulus of Elium during the polymerization cycle

The plots the trends of the normalized storage modulus (E0) and the loss tangent (tanδ) are represented as a function of temperature. This test allows the detection of all the thermal transitions of the tested specimens in the selected temperature range. Elium has a high amount of volumetric shrinkage up to 13% with having storage modulus 1MPa. [33]

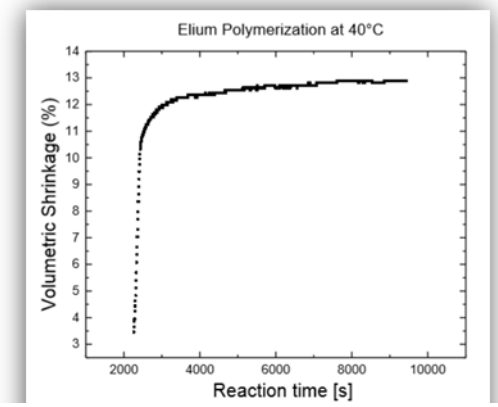

$$\varepsilon_v = \left[1 + \frac{1}{3}\left(\frac{h - h_0}{h_0}\right)\right]^3 - 1$$

h = gap height
h_o = initial gap height

Fig. 2.10: Volumetric Shrinkage change in Elium resin during the polymerization cycle

2.2.7 Cone Calorimeter Test

Heat release and smoke production behavior of the composites were analyzed on a cone calorimeter fabrics were placed between two layers of FR (flame retardant) mats. Sample dimensions of 100 mm × 100 mm were exposed to a heat flux of 35 kW/m2 in accordance with ISO 5660–1 graphene nano-platelet. The FR composites were designated after their commercial mat grades, namely, E20MI, E11MIL, T6663 and T6594. The Control composite without the FR coating mats was produced for comparison of properties. [35]

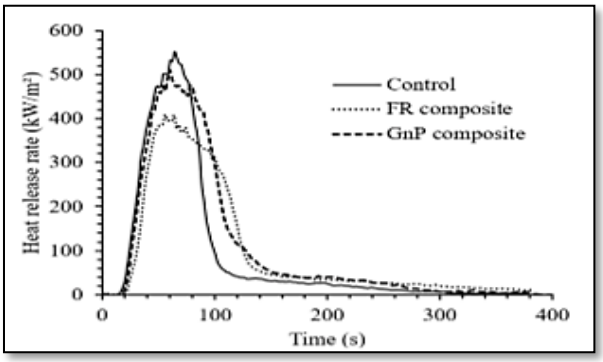

Fig. 2.11: Heat release rate in Elium resin during the polymerization cycle

2.2.8 Differential Scanning Calorimetry (DSC)

To study the influence of the peroxide initiator in the polymerization, differential scanning calorimetry (DSC) is a thermo analytical technique in which the difference in the amount of heat required to increase the temperature of a sample and reference is measured as a function of temperature.

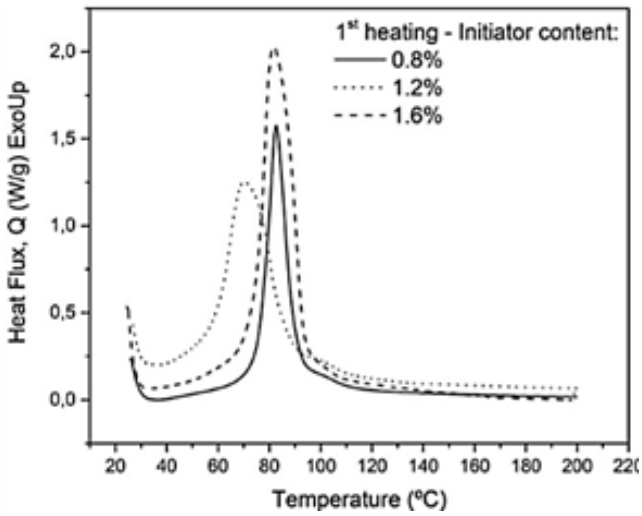

Fig. 2.12: Heat Flux of Elium during differential scanning calorimetry (DSC)

Samples with 0.8% and 1.6% initiator contents present no significant variation in the onset temperature values, and the reaction in both cases starts at approximately 75°C. Total heat of the reaction is dependent on the molecular weight of the formed chains. The theoretical heat of polymerization of MMA is −550 J/g. [36]

Initiator content in weight (%)	T_{onset} (°C)	T_{max} (°C)	$-\Delta H$ (J/g)
0.8	75.9	82.6	129.4
1.2	57.9	70.4	150.7
1.6	74.0	81.8	210.7

Table. 2.3: Differential scanning calorimetry (DSC) test for Elium resin

2.2.9 Degree Of Conversion (DOC)

Conversion or polymerization degree (α) calculated as a function of the temperature (T). The results for each initiator concentration are presented in Figure. [36]

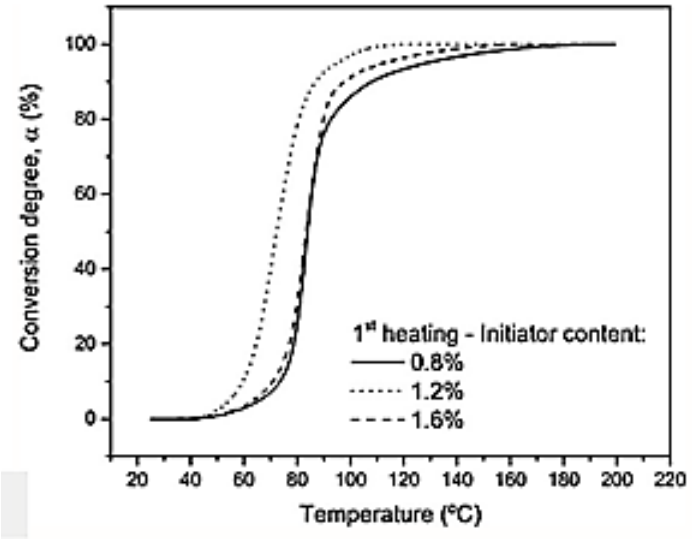

Fig. 2.13: Degree of Cure for Elium resin with percentage of initiator

The three curves present two plateaus separated by an exponential growth region. Even though the DSC results do not allow the determination of the exact limit between the polymerization reaction steps, it is reasonable to assume that the first plateau is mainly associated with the induction period that precedes the initiation and propagation of the reaction. This latter propagation stage is, therefore, represented by the exponential growth region, which takes place until reaching its termination at the second plateau.

Initiator content in weight (%)	T_{gDSC} (°C)
0.8	97.7
1.2	95.8
1.6	90.0

Table. 2.4: Gel Point for Elium resin with percentage of initiator

2.2.10 Thermo Gravimetric Analysis (TGA)

Thermo gravimetric analysis (TGA) and DTG curves are presented in Figure 8 for all three samples with 0.8%, 1.2%, and 1.6% in mass content of initiator. [36]

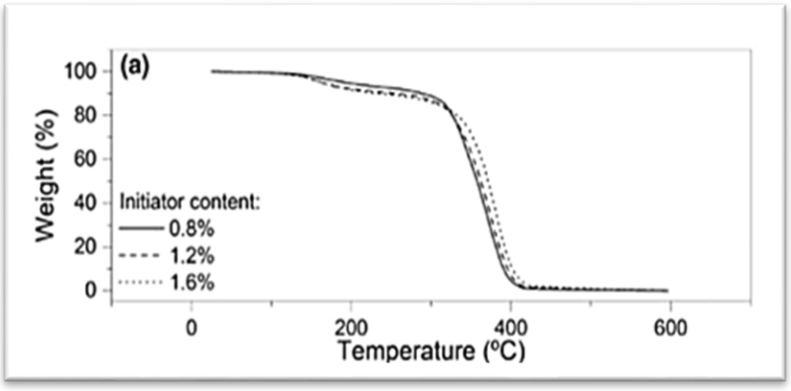

Fig. 2.14: Loss in weight for Elium resin w.r.t temperature

From these curves it can be noticed that the three samples present only minor differences in the decomposition behavior. DTG is a type of thermal analysis in which the rate of material weight changes upon heating is plotted against temperature and used to simplify reading the weight versus temperature thermogram peaks which occur close together The thermal decomposition, regardless the initiator content, occurred in two stages and was completed in temperatures below 500°C, reaching 100% in weight loss.

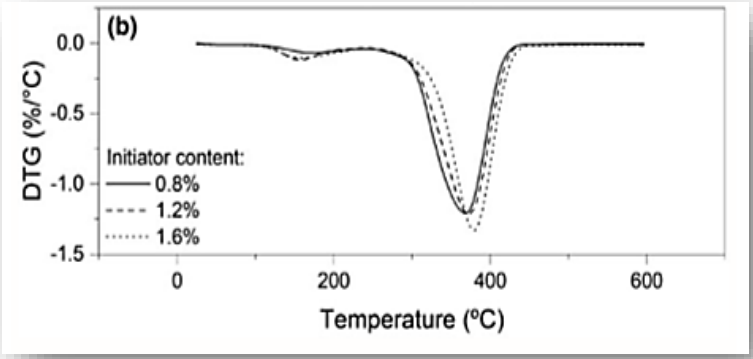

Fig. 2.5: Derivative Thermo Gravimetric (DTG) for Elium resin with percentage of initiator

Chapter#3

3 Manufacturing of Wind Blade

Composite materials are used typically in blades and nacelles of wind turbines. Generator, tower, etc. are manufactured from metals. Blades are the most important composite based part of a wind turbine, and the highest cost component of turbines. A wind turbine blades consists of two faces (on the suction side and the pressure side), joined together and stiffened either by one or several integral (shear) webs linking the upper and lower parts of the blade shell or by a box beam (box spar with shell fairings) (see Schema on Fig. 3.1) [37]. The flap wise load is caused by the wind pressure, and the edgewise load is caused by gravitational forces and torque load. The flap wise bending is resisted by the spar, internal webs or spar inside the blade, while the edges of the profile carry the edgewise bending. From the point of loads on materials, one of the main laminates in the main spar is subjected to cyclic tension-tension loads (pressure side) while the other (suction side) is subjected to cyclic compression-compression loads. The laminates at the leading and trailing edges that carry the bending moments associated with the gravitation loads are subjected to tension-compression loads. The aero shells, which are made of sandwich structures, are primarily designed against elastic buckling. The different cyclic loading histories that exist at the various locations at the blades suggest that it could be advantageous to use different materials for different parts of the blade.

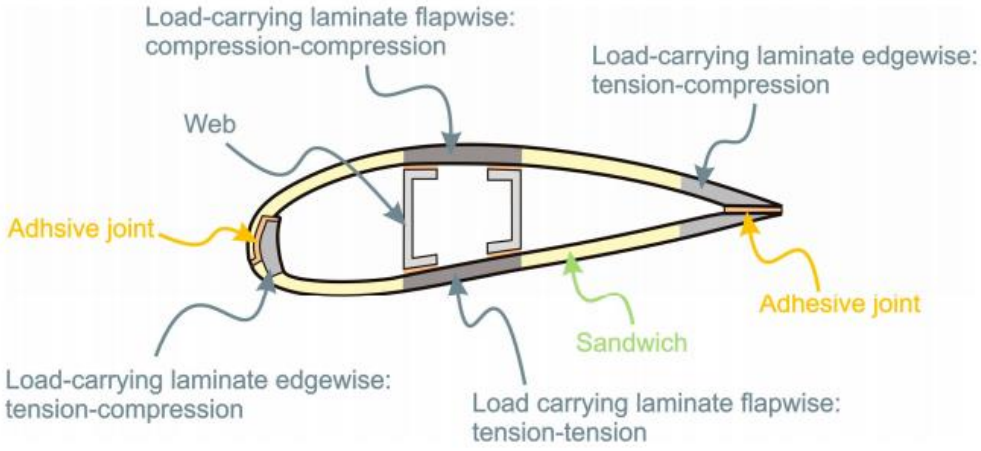

Fig. 3.1: Cross section of the wind turbine blade

3.1 Overview of the Manufacturing Process

During the first decades of the wind energy development, wind turbine blades were often produced using the wet hand lay-up technology, in open molds. The glass-fiber reinforcement was impregnated using paint brushes and rollers. The shells were adhesively bonded together/to the spars. This technology was used mainly to produce small and medium size blades (up to 35 and 55 m, respectively). For larger blades, the same technology was used, but the web was inserted and adhesively bonded between two sides, and the plies with more fiber content were used. The disadvantages of the open mold technology are high labor costs, relatively low quality of products and environmental problems. In 1970s, several companies and institutes explored the applicability of filament winding technology, seeking to improve the quality of turbine and to reduce labor costs [38]. The introduction of vacuum infusion and prepreg technologies allowed improving the quality of manufacturing [39]. The prepreg technology, adapted from the aircraft industry, is based on utilizing "pre-impregnated" composite fibers, which already contain an amount of the matrix material bonding them together. Prepreg (widely used, for instance, by the Danish wind turbine producer Vestas) allows the industrial impregnation of fibers, and then forming the impregnated fibers to complex shapes. The most widely used technology to produce the wind blades, especially longer blades, is the resin infusion technology. In the resin infusion technology, fibers are placed in closed and sealed mold, and resin is injected into the mold cavity under pressure. After the resin fills all the volume between fibers, the component is cured with heat. The resin infusion technologies can be divided into two groups: Resin Transfer Molding (RTM) (resin injection under pressure higher than atmospheric one) and Vacuum Assisted Resin Transfer Molding (VARTM) (or Vacuum Infusion Process) (when resin is injected under vacuum or pressure lower than atmospheric, typically, under a vacuum bag) [40]. A variation of VARTM called SCRIMP™ (i.e., Seemann Composite Resin Infusion Process) was developed in late 1980s and is quite efficient for producing large and thick parts. Currently, vacuum assisted resin transfer molding (VARTM) is the most common manufacturing method for manufacturing of wind turbine rotor blades. With his method, layers of fabrics of dry fibers, with nearly all unidirectional fibers, aligned in the direction along the length of the blade, are position on mold parts along with polymer foams or balsa wood for sandwich structures (for the aero shells). In order to form a laminate that

is thick by the root and gradually becomes thinner towards the tip, most plies run from the root only partly toward the tip; the termination of a ply is called ply-drop. The fabrics and subsequently covered by a vacuum bag and made air-tight. After the application of vacuum, low-viscosity resin flows in and wets the fibers. After infusion, the resin cures at room temperature. In most cases, wind turbine rotor blades are made in large parts, e.g., as two aero shells with a load-carrying box (spar) or internal webs that are then bonded together. Sometimes, the composite structure is post cured at elevated temperature. In principle, this manufacturing method is well suited for upscaling, since the number of resin inlets and vacuum suction points can be increased. A challenge with upscaling is however, then quite many layer of dry fabrics must be kept in place and should not slip relative to each other. The composite is quite thick by the root section, typically exceeding 50–60 mm in the consolidated state. In practice, it can be a challenge to avoid the formation of wrinkles at double-curved areas and areas with un-wetted fibers and air bubbles can be entrapped in the bond lines. After manufacturing, the blades are subjected to quality control and manufacturing defects are repaired. Since a large blade represents a large value in materials, increasing sizes means that it becomes less and less attractive to discard blades with manufacturing defects. Thus, with increasing size the requirements towards materials go towards easier processing and materials should preferably be more damage tolerant so that larger manufacturing defects can be tolerated. Fig. 3.1.1 shows the schematics of the manufacturing of a wind turbine rotor blade by assemblage and bonding of two aero shells and two shear webs. The infusion process is usually cheaper that the prepreg process. However, the prepreg composites have more stable, better and less variable mechanical properties than the composites produced by resin infusion. This technology is relatively environmental friendly, and makes it possible to achieve higher volume content of fibers, and to control the materials properties. Further, the prepreg technology allows higher level of automation and better choice of resins. Lately, the automated tape lay-up, automated fiber placement, two-pieces or segment wind blades, enhanced finishing technologies are expected to come into use to improve quality and reduce costs of the composite blade manufacturing [39]. A big challenge, in comparison with e.g., automatization of composite structures for aerospace, is the much larger thicknesses and the much larger amount of materials to be places in the molds for wind turbine rotor blades. For some parts of the blades,

3D woven composites represent a promising alternative to producing fiber reinforced laminates. Mohamed and Wetzel [41] suggested producing spar caps from 3D woven carbon/glass hybrid composites. It was demonstrated that this technology allows producing spar caps with higher stiffness and lower weight, than the commonly used technologies.

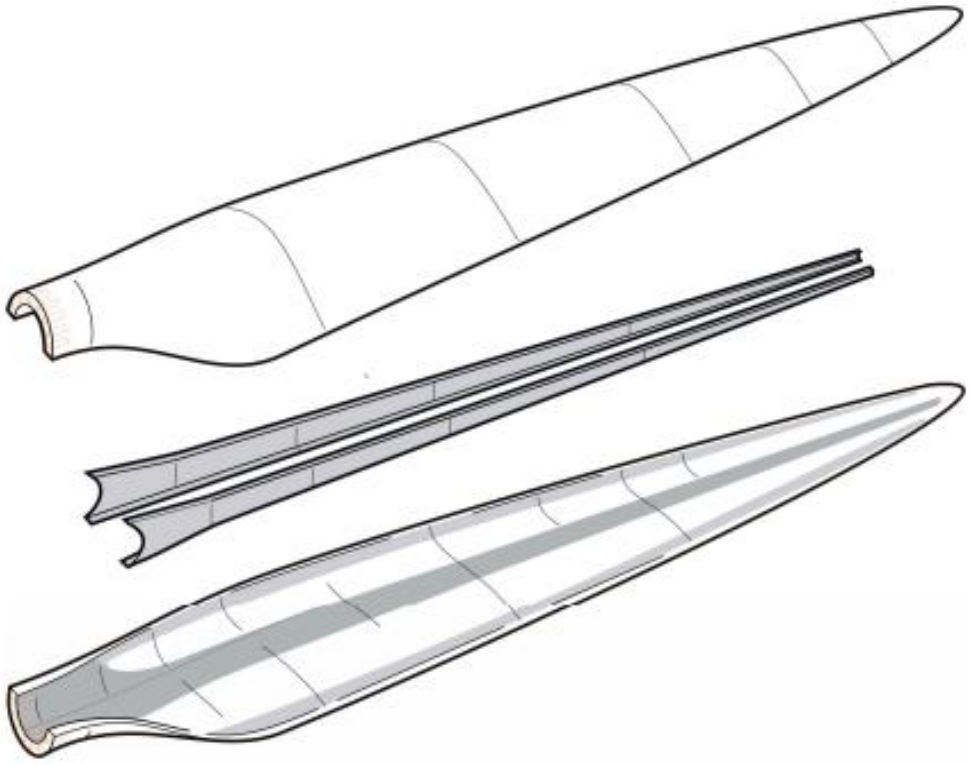

Fig. 3.2: Manufacturing of a wind turbine rotor blade by assemblage and bonding of two aero shells and two shear webs.

The infusion process is usually cheaper that the prepreg process. However, the prepreg composites have more stable, better and less variable mechanical properties than the composites produced by resin infusion. This technology is relatively environmental friendly, and makes it possible to achieve higher volume content of fibers, and to control the materials properties. Further, the prepreg technology allows higher level of automation and better choice of resins.

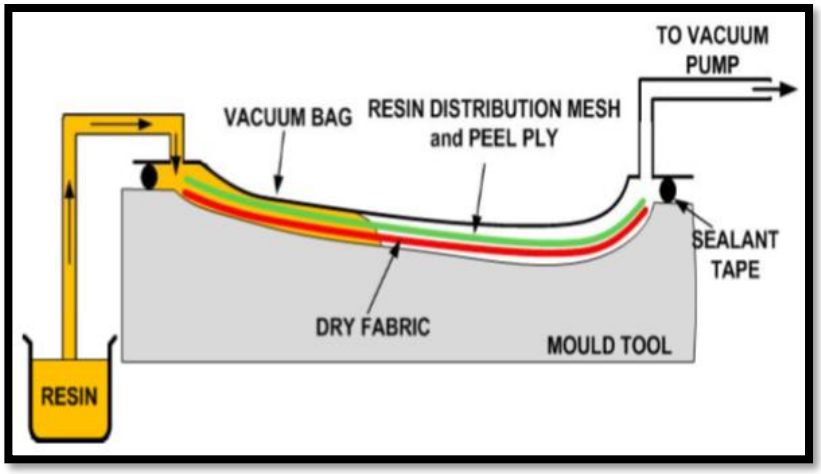

Fig. 3.3: Manufacturing of outer shell of wind turbine blade

Based on RTM manufacturing principles, the vacuum infusion technique uses a solid mold half and a flexible mold half (usually a plastic film) instead of a set of two solid mold halves. Due to the flexible mold half, processing pressure is limited to atmospheric pressure.

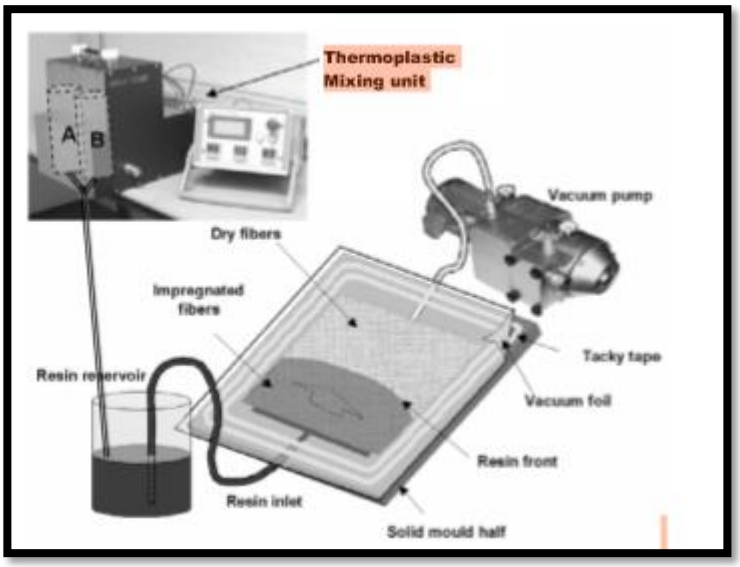

Fig. 3.4: Manufacturing apparatus of Vacuum Infusion Process [42]

As with RTM, the first step of the process involves placing a dry fiber pre-form on the surface of the solid mold half (see Figure). The second step consists of covering the mold with a flexible medium, in this case, either a vacuum bag or a semi-rigid mold half (also known as light RTM). Once the vacuum is pulled between the flexible and the solid mold

halves, the resin system can be introduced by opening an inlet valve. Resin is then forced to flow toward the outlet port connected to the vacuum pump. Once the pre- form is fully impregnated, the inlet port is closed and the part is left to polymerize before being released from the mold. As with RTM, isothermal or non-isothermal processing is possible depending on the resin system. In all cases, the resin reservoirs must be kept above the melting temperature of the different components of the polymer reactive system and the mold must be kept at the polymerization temperature. Compared to RTM, vacuum infusion has the advantage of being low-cost and allows the manufacture of significantly larger parts. However, infusion time is longer due to low processing pressure and poor surface finish will always be obtained on the flexible mold side. Also, since vacuum bags and other consumables are generally not reusable, the process should be considered less sustainable. Vacuum infusion of thermoplastic composites has also not yet been used on an industrial scale, but different systems and manufacturing techniques were investigated over the past decade. Significant progress in process development for anionic polyamide-6/glass composites was achieved at Delft Technical University [43] and infusion of APA-6 on carbon fibers was investigated at the University of Alabama [44].

3.2 Blade Components & Fiber Orientation

Wind turbine blades are being manufactured using PMC, in a combination of monolithic (single skin) and sandwich composites. The composites laminated parts are either glass or carbon fiber-reinforced polymers, while the sandwich core materials may be polymeric foams (PVC or BMI), balsa wood core or less frequently of honeycomb type (nomex). Considering the layout of wind turbine blades, the following design feature are typically adopted:

Outer shells: Composite sandwich laminates towards leading and trailing edges to increase the buckling resistance (edgewise loading). With the traditional blade design, see Figures below, the sandwich shell parts are transferred into relatively thin monolithic composite laminates in the areas where the shells are adhesively bonded to the main spar. For the internal web/stiffener blade design, see below.

Main spar flange: The main spar usually extends from the root of the blade to a position close to the tip. As mentioned, the primary function of the main spar is to transfer the blade wise bending load, and thus it has to perform as a beam. The primary function of the flanges is to carry the flap wise bending moment, and they are usually made as thick monolithic composite laminates, which for some large blades is made using hybrid glass/carbon composites. The main spar lay-up usually includes UD-layers to provide for the bending stiffness as well as off-axis or angle-ply layers to provide for the buckling resistance of the flange loaded in compression (suction side of airfoil). The function of the webs is to carry the flap wise shear forces, and they are usually made as composite sandwich plates with polymeric or balsa core and with thin composite face sheets (±45° orientation relative to blade length coordinate).

Spar cap: The primary function of the spar cap section is to carry the flap wise bending moment, and it is usually made as a thick monolithic composite laminate, which for some large blades is a hybrid glass/carbon composite. The carbon fibers are used to enhance the bending stiffness of the blade. The main spar lay-up usually includes UD-layers to provide for the bending stiffness as well as off-axis or angle-ply layers to provide for the buckling resistance of the flange loaded in compression (suction side of airfoil).

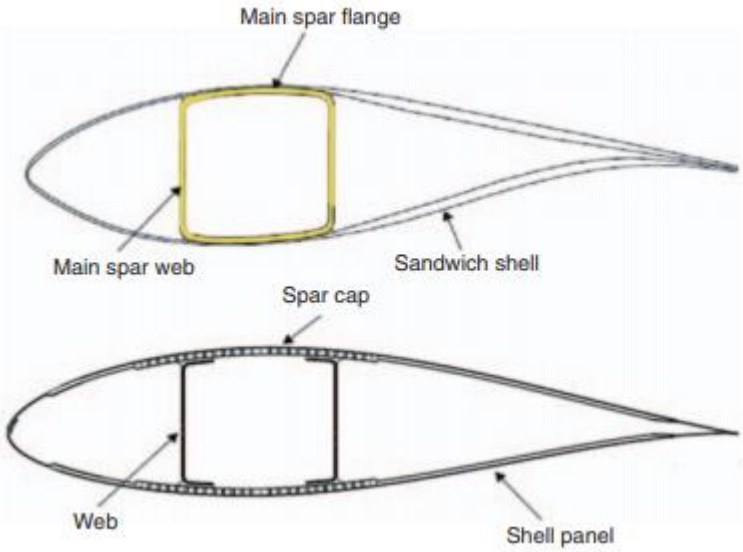

Fig. 3.5: Description of the wind turbine blade layout and its components

Internal webs/stiffeners: The function of the webs is to carry the flap wise shear forces, and they are usually made as composites and which plates with polymeric or balsa core and relatively with biax laminate thin composite face sheets (±45° orientation relative to blade length coordinate). The sandwich design is chosen in order to enhance the resistance against in-plane shear buckling.

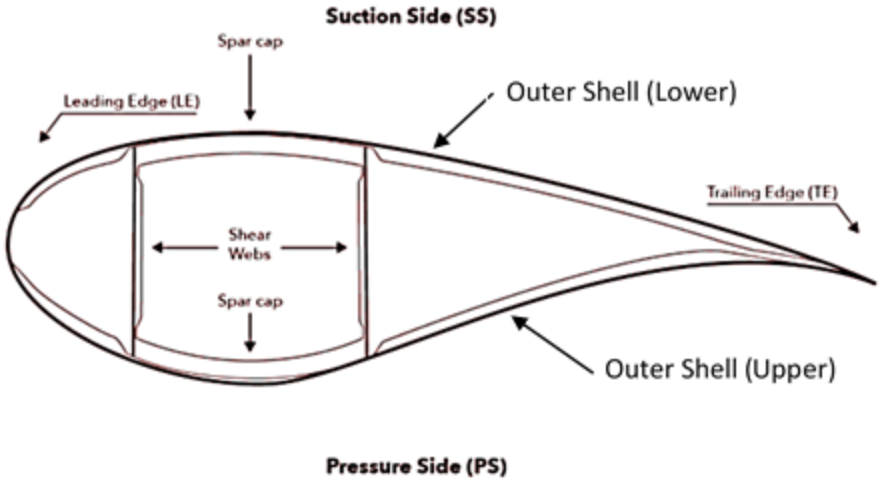

Fig. 3.6: Labelling of the wind turbine blade

Fiber orientation is usually considered while manufacturing wind blades [45], because they become highly resistant to shear forces and the transversal unidirectional plies are incorporated to sustain compressive forces. Biaxial, tri-axial and unidirectional fabrics are used in the construction of the blades that are composed by flanges, shear webs, top and button skins, root and others as shown in Fig. below which presents the fiber orientation configuration, which is possible for the design of the multilayered composite blade. Fiber orientation is usually considered while manufacturing wind blades [45], because they become highly resistant to shear forces and the transversal unidirectional plies are incorporated to sustain compressive forces. Biaxial, tri-axial and unidirectional fabrics are used in the construction of the blades that are composed by flanges, shear webs, top and button skins, root and others as shown in Fig. below which presents the fiber orientation configuration, which is possible for the design of the multilayered composite blade.

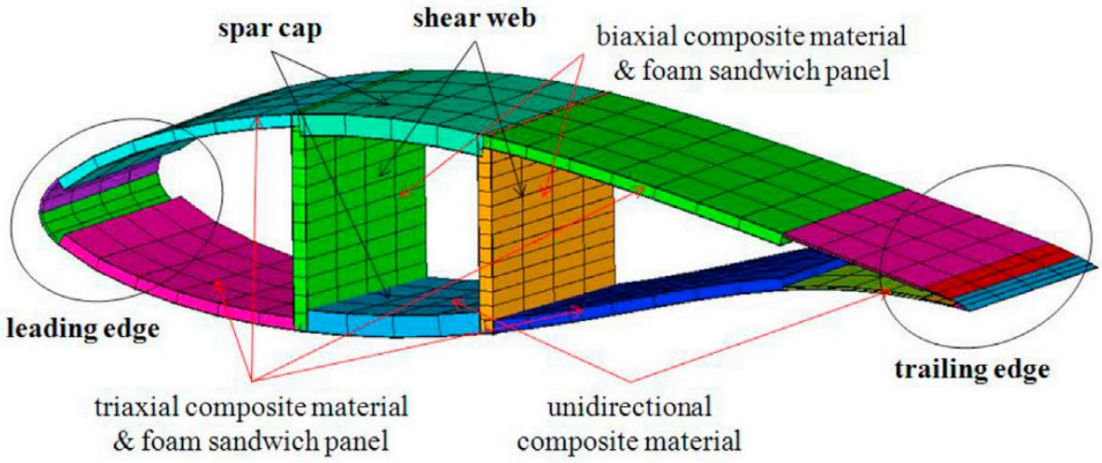

Fig. 3.7: Fiber orientation across the various cross section of wind turbine blade

3.3 Manufacturing with Thermosets

Thermosets based composites represent around 80% of the market of reinforced polymers. The advantages of thermosets are the possibility of room or low temperature cure, and lower viscosity (which eases infusion and thus, allowing high processing speed). Initially, polyester resins were used for composite blades. With the development of large and extra-large wind turbines, epoxy resins replaced polyester and are now used most often as matrices of wind blade composites. Still, recent studies (e.g., by Swiss company DSM Composite Resins) support arguments for the return to unsaturated polyester resins, among them, faster cycle time and improved energy efficiency in the production, stating that the newly developed polyesters meet all the strength and durability requirements for large wind blades. Further, the development of matrix materials which cure faster and at lower temperatures is an important research area.

3.4 Manufacturing with Thermoplastics

Thermoplastics represent an interesting alternative to the thermoset matrices. The important advantage of thermoplastic composites is their recyclability. Their disadvantages are the necessity of high processing temperatures (causing the increased energy consumption and possibly influencing fiber properties) and, difficulties to manufacture large (over 2 m) and thick (over 5 mm) parts, due to the much higher viscosity. The melt viscosity of

thermoplastic matrices is of the order 102–103 Pa s, while that for thermosetting matrix is around 0.1–10 Pa s. Thermoplastics (as differed from thermosets) have melting temperatures lower than their decomposition temperatures, and, thus, can be reshaped upon melting. While the fracture toughness of thermoplastics is higher of thermosets, fatigue behavior of thermoplastics is generally not as good as thermosets, both with carbon or glass fibers [46]. Other advantages of thermoplastics include the larger elongation at fracture, possibility of automatic processing, and unlimited shell life of raw materials.

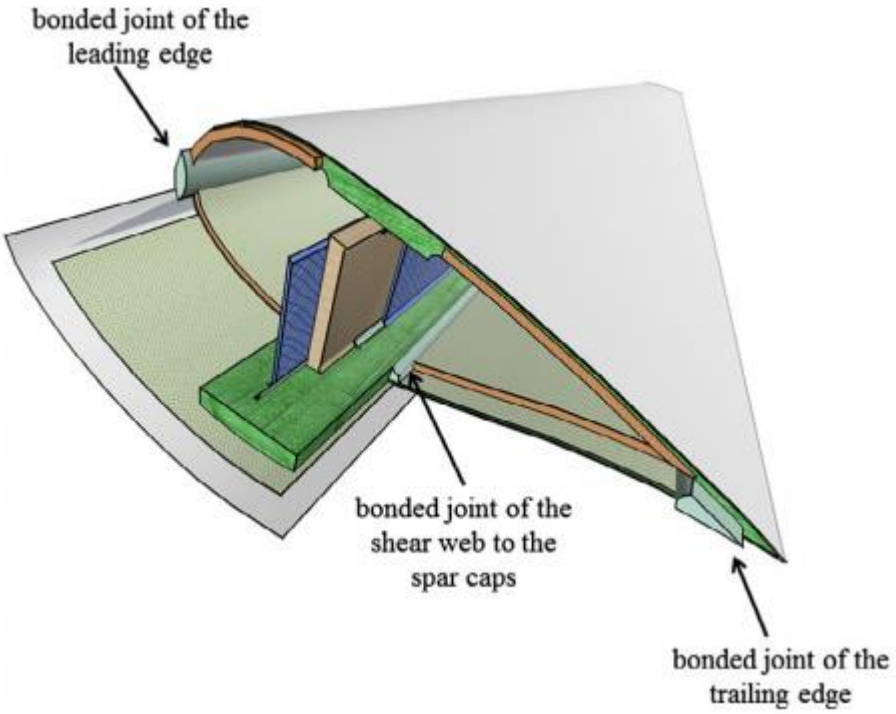

Fig. 3.8: Cross section of the wind turbine blade with thermoplastic composite laminates and bonding joints

Chapter # 4

4 Process Modelling of Wind Blades

The production of rotor blades for wind turbines is still a predominantly manual process. Process simulation is an adequate way of improving blade quality without a significant increase in production costs. This paper introduces a module for tolerance simulation for rotor-blade production processes. The investigation focuses on the simulation of temperature distribution for one-sided, self-heated tooling and thick laminates. Experimental data from rotor-blade production and down-scaled laboratory tests are presented. Based on influencing factors that are identified, a physical model is created and implemented as a simulation. This provides an opportunity to simulate temperature and cure-degree distribution for two-dimensional cross sections. The aim of this simulation is to support production processes. Hence, it is modelled as an in situ simulation with direct input of temperature data and real-time capability. A monolithic part of the rotor blade, the main girder, is used as an example for presenting the results.

4.1 Introduction

The production of rotor blades for wind turbines is still a predominantly manual process. In order to improve blade quality without a significant increase in production costs, tolerance management is combined with statistical process control. A process model with both analytical and numerical elements is developed, based on statistical production data and experiments. The investigation presented here focuses on the simulation of temperature distribution for one-sided, self-heated tooling and thick laminates. The model includes the properties of the heating system and the exothermic behavior of resin. The simulation is linked to experiments with varying process temperatures and laminate thicknesses. Even if the geometry of rotor blades is not as complex as an airplane wing cover, different zones have to be taken into account. In Fig. 4.1 below, a generic cross section of a rotor blade is shown. The main, girders (yellow), and possibly minor girders, are made of unidirectional glass or carbon-fiber reinforced plastics. Non-crimped fabric, pre-impregnated fibers or roving can be used as raw materials according to the company-specific production process.

As the girders take the main bending loads, the laminate quality of these parts is crucial. Torsional loads are carried by the shells and shear webs (turquoise). Therefore, a higher moment of inertia is required. In order to achieve this without unnecessary weight gain, sandwich material is used for shells and shear webs. Thin glass-fiber top layers cover a polyethylene terephthalate (PE/PET) foam core. Sometimes, in regions of higher loads, balsa core material is also used.

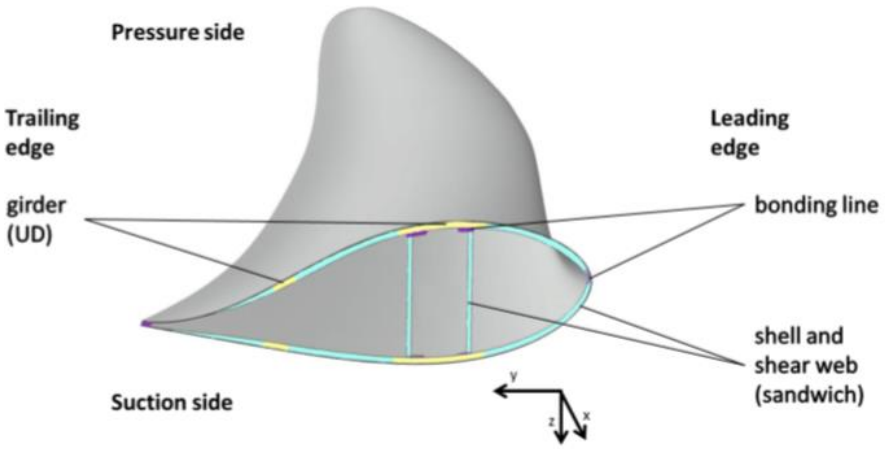

Fig. 4.1: Typical cross section of a rotor blade according to [47-49].

The girders are prefabricated parts and connected with the shells by the infusion process (Fig. 4.2). Shells are joined to each other and with the shear webs in a bonding process with thixotropic adhesives for secondary bonding lines (purple).

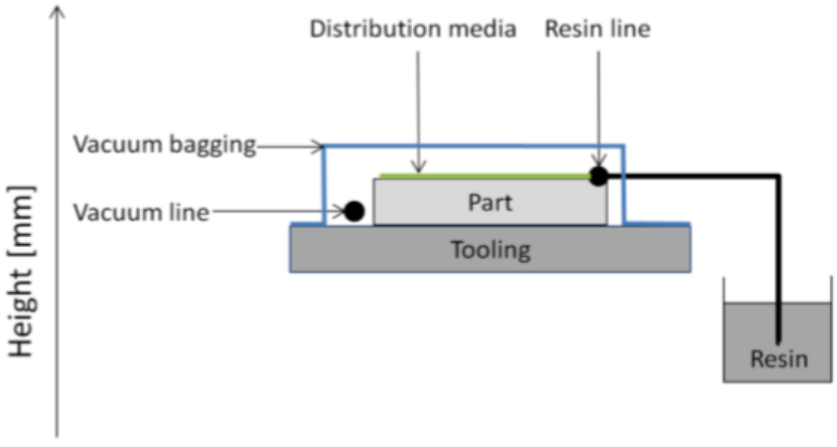

Fig. 4.2: Vacuum-assisted resin infusion (VARI) procedure according to [50-51].

A general structure of a rotor blade middle section, including the material distribution described, is summarized in Fig. 4.1. The Fig. 4.1 only shows the outer (tip) section of a rotor blade. In the root section are zones with wall thicknesses of up to 100 mm made of triaxial glass-fiber composite for the load transfer between blade and hub. The production process of rotor blades includes the prefabrication of girders, shear webs, parts of root sections, and additional smaller parts. These are joined to the suction or pressure side shell, respectively, by a liquid resin infusion process. In most cases, the shear webs (one or more) are bonded to one shell and cured. Blind bonding is the final production step of the blade blank. Here, the shells and the shear webs are connected to a closed rotor blade. The central production step for manufacturing fiber-reinforced plastics for wind-turbine applications is the infusion process. As each manufacturer has their own special features, Fig. 4.2 shows a general overview of a vacuum-assisted resin infusion (VARI) process. In Fig. 4.2, a generic part of dry fabric is impregnated with epoxy resin. For rotor blades, in the majority of cases non-woven fabric is used. The infusion is driven by pressure differences between the low pressure in the cavity of the part (evacuated by vacuum line) and the resin reservoir under ambient pressure. The filling ratio, the fiber volume faction, is achieved by the equilibrium of forces between the resin reservoir and part compaction. For complete filling, the resin is spread by the resin line and a distribution media on the top surface of the component. Due to the part's large dimensions, tooling is one-sided, with an integrated heating system. The resulting challenge is achieving the temperature gradient between tooling and part surface, which becomes more significant with rising wall thicknesses and isolation materials. The resins used are mostly epoxy-based. To achieve an acceptable occupancy time for tooling, they are cured at temperatures of about 80 ◦C. During this curing process, the epoxy resin's reaction is exothermic. This poses a process risk that the resin's limit temperature will be exceeded. Due to the laminate's low thermal conductivity, this risk increases with the thickness of laminates, which need to be reduced. Through the prediction of process temperatures, thermal damage to parts due to the melting of auxiliary materials, process-induced deformations [52] or laminate characteristics [53], can be avoided. Therefore, a simulation module for predicting the process temperatures in fiber-reinforced plastics with one-sided, heat able molds is required.

4.2 Application of Classical Laminate Theory

Classical Lamination Theory (CLT) is a commonly used predictive tool, which evolved in the 1960s, which makes it possible to analyze complex coupling effects that may occur in composite laminates. It is able to predict strains, displacements and curvatures that develop in a laminate as it is mechanically and thermally loaded. The method is similar to isotropic plate theory, with the main difference appearing in the lamina stress-strain relationships.

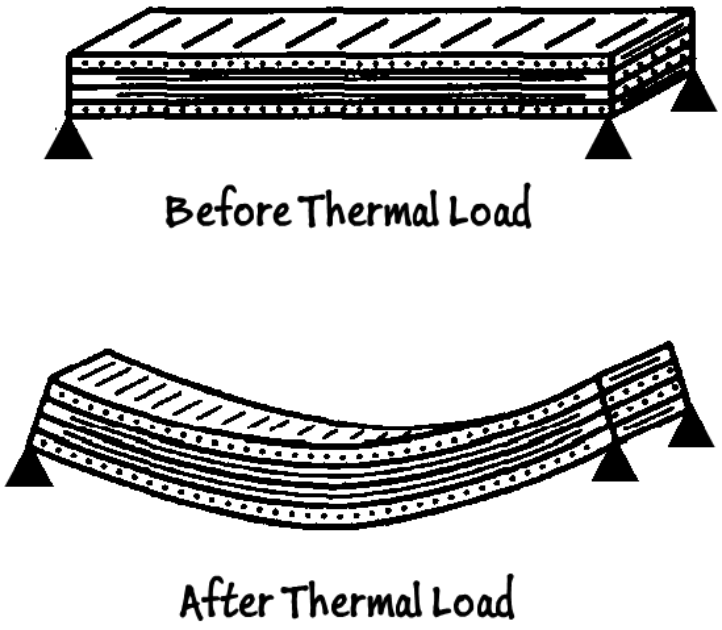

Fig. 4.3: Composite laminate before and after the application of thermal laod

4.2.1 Hooke's law utilization in CLT

The Generalized Hooke's Law of stress and strain of any material is,

$$\begin{Bmatrix} \sigma_x \\ \sigma_y \\ \tau_{xy} \end{Bmatrix} = \begin{bmatrix} \overline{Q_{11}} & \overline{Q_{12}} & \overline{Q_{16}} \\ \overline{Q_{12}} & \overline{Q_{22}} & \overline{Q_{26}} \\ \overline{Q_{16}} & \overline{Q_{26}} & \overline{Q_{66}} \end{bmatrix} \begin{Bmatrix} \varepsilon_x \\ \varepsilon_y \\ \gamma_{xy} \end{Bmatrix} \qquad \textit{Eq. 4.1}$$

Where is the stiffness matrix Q, are stress components σ, are strain components ε. The Generalized Hooke's Law for an Orthotropic Material reduces to;

4.2.2 Assumptions for Classical Laminate Theory

As with any analytical technique, some assumptions must be made in order to make the problem solvable:

1. The plate consists of orthotropic lamina bonded together, with the principal material axes of the orthotropic lamina orientated along arbitrary directions with respect to the x-y axes.
2. The thickness of the plate, t, is much smaller than any characteristic dimension.
3. The displacements u, v, and w are small compared with t.
4. The in-plane strains ε_x, ε_y, and γ_{xy} are small compared with unity.
5. Transverse shear is negligible, $\gamma_{xz} = \gamma_{yz} = 0$ (plane stress in each ply).
6. Displacements u and v are assumed to be linear functions of the thickness coordinate z (no warping).
7. Assumptions 5 and 6 together define the Kirchhoff hypothesis.
8. Transverse normal strain ε_z is negligible.
9. Each ply obeys Hooke's Law.
10. The plate thickness is constant throughout the laminate.
11. Transverse shear stress τ_{xz} and τ_{yz} vanish on the laminate surfaces z = ± t/2.

These assumptions lay the foundation for the theory and enable prediction of composite laminate behavior. More details will follow, so that we can understand the modifications made to the existing methodology.

4.2.3 Hooke's Law for Lamina under plane stress state

A thin plate is a prismatic member having a small thickness, and it is the case for a typical lamina. If a plate is thin and there are no out-of-plane loads, it can be considered to be under plane stress. If the upper and lower surfaces of the plate are free from external loads, then, and. This assumption then reduces the three dimensional stress–strain equations to two-dimensional stress–strain equations.

A unidirectional lamina falls under the orthotropic material category. If the lamina is thin and does not carry any out-of-plane loads, one can assume plane stress conditions for the

lamina. Therefore, taking, and, Equation for an orthotropic plane stress problem can then be written as (4.2) Inverting Equation stress–strain relationship is, (4.3)

$$\begin{Bmatrix} \sigma_x \\ \sigma_y \\ \tau_{xy} \end{Bmatrix} = \begin{bmatrix} \overline{Q_{11}} & \overline{Q_{12}} & 0 \\ \overline{Q_{12}} & \overline{Q_{22}} & 0 \\ 0 & 0 & \overline{Q_{66}} \end{bmatrix} \begin{Bmatrix} -\alpha_x \Delta T \\ -\alpha_y \Delta T \\ -\alpha_{xy} \Delta T \end{Bmatrix} \quad \textit{Eq. 4.2}$$

Where are the reduced stiffness coefficients, which are related to the Compliance coefficients as Stiffness coefficients in terms of engineering or technical constants is

$$[T] = \begin{bmatrix} m^2 & n^2 & 2mn \\ n^2 & m^2 & -2mn \\ -mn & mn & m^2 - n^2 \end{bmatrix}; \quad \textit{Eq.4.3}$$

$$[Q] = [T]^{-1} \begin{bmatrix} \overline{Q_{11}} & \overline{Q_{12}} & \overline{Q_{16}} \\ \overline{Q_{12}} & \overline{Q_{22}} & \overline{Q_{26}} \\ \overline{Q_{16}} & \overline{Q_{26}} & \overline{Q_{66}} \end{bmatrix} [T]; \{\varepsilon\} = [T] \begin{Bmatrix} \varepsilon_x \\ \varepsilon_y \\ \gamma_{xy} \end{Bmatrix} \quad \textit{Eq. 4.4}$$

The coordinate system used for showing an angle lamina is as given in Fig. The angle between the two axes is denoted by an angle θ. Fig: Angle lamina showing local and global axes Relation between stress and strain in global axis is, where are called the elements of the transformed reduced stiffness matrix, from above equations, it can be seen that they are just functions of the four stiffness elements, and the angle of the lamina, θ.

4.2.4 Stress Distribution in Symmetric and Non-Symmetric Laminate

Based on the earlier calculation work, graphs for symmetric and non-symmetric laminates would be plot like this;

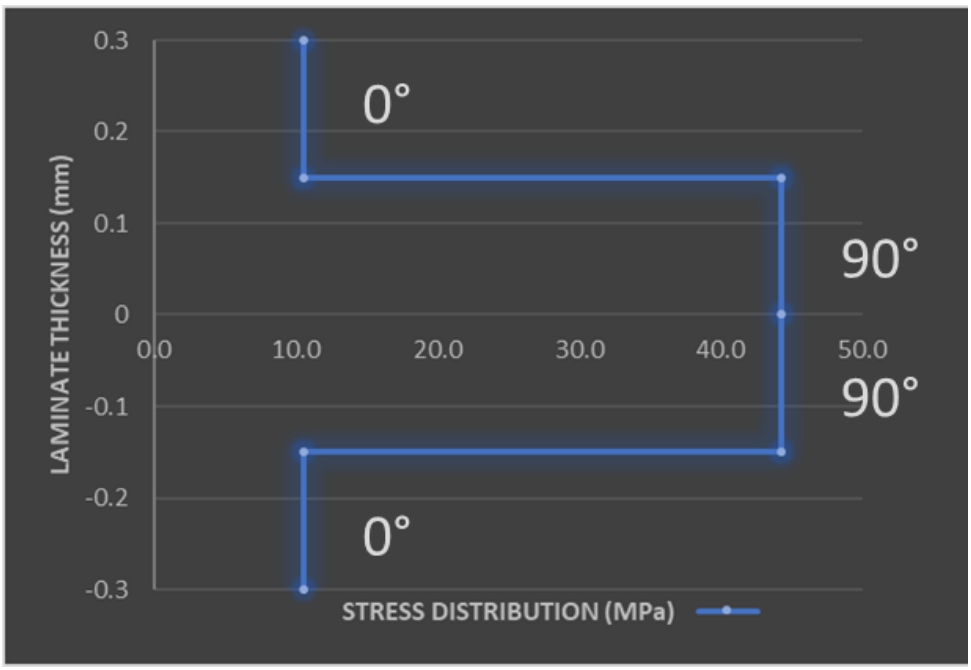

Fig. 4.4: Stress distribution in case of thermal load in [0/90] s laminate

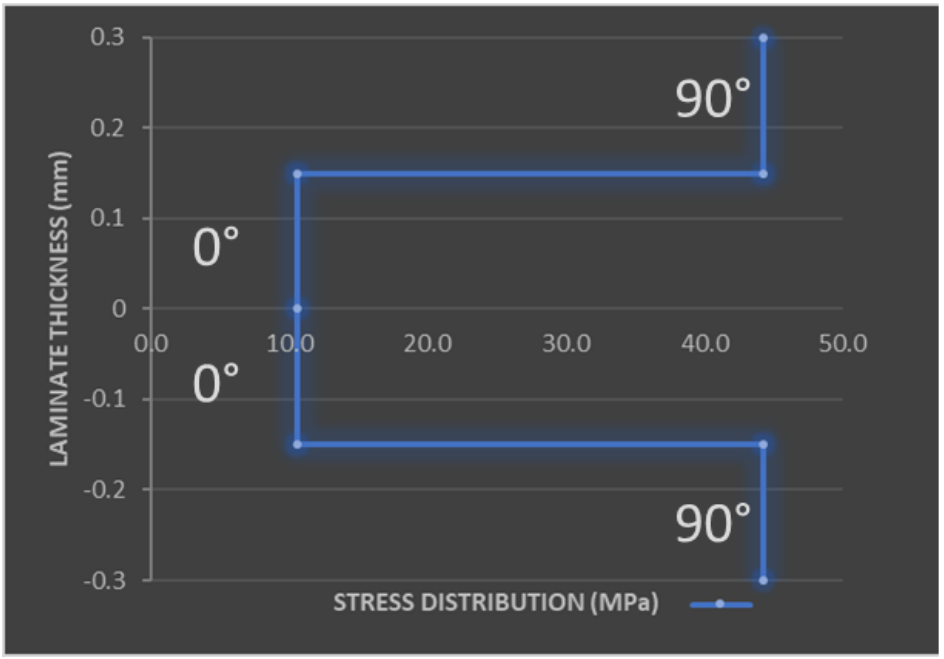

Fig. 4.5: Stress distribution in case of thermal load in [90/0] s laminate

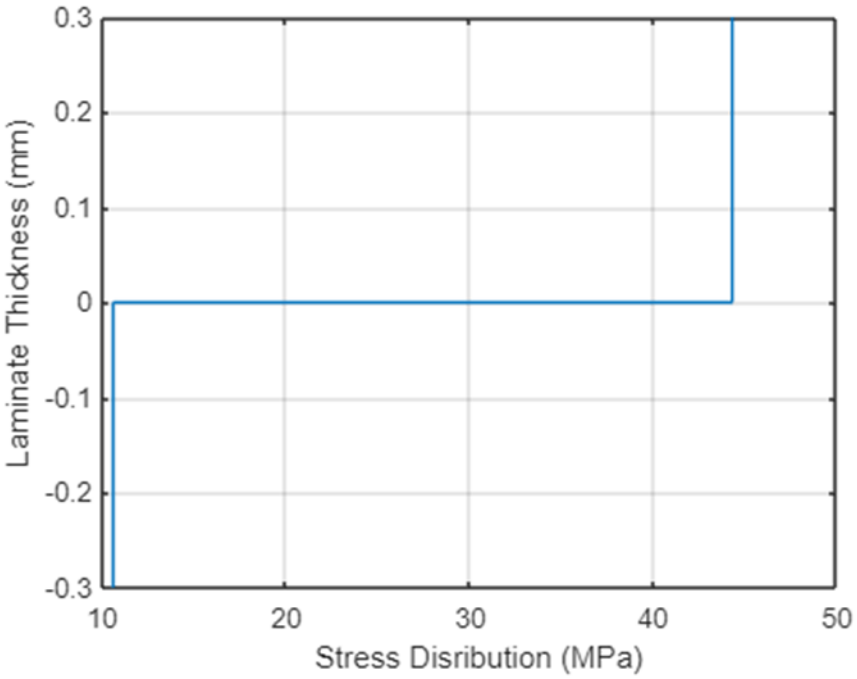

Fig. 4.6: Stress distribution in case of thermal load in [0/90] non symmetric laminate

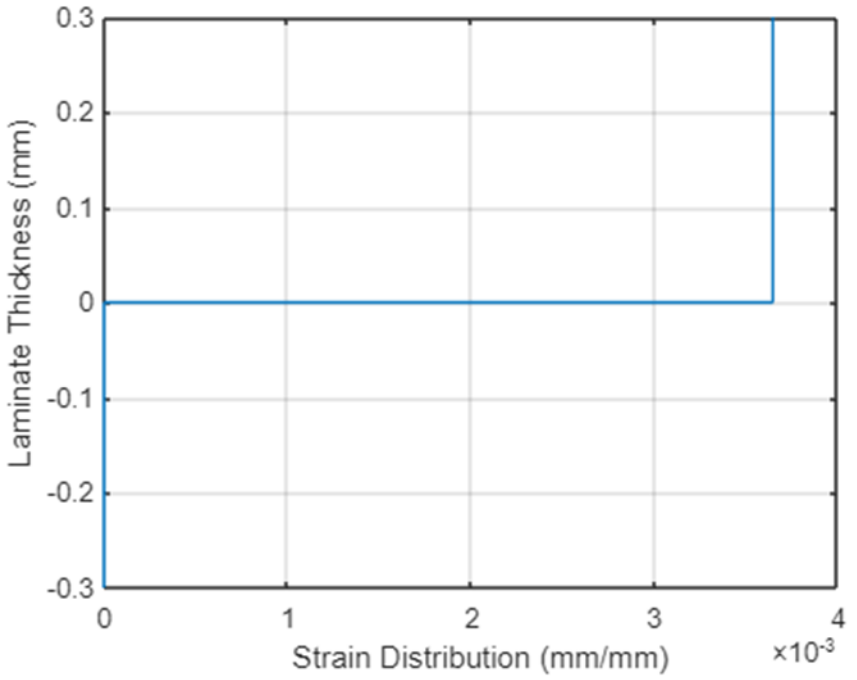

Fig. 4.7: Strain distribution in case of thermal load in [0/90] non symmetric laminate

4.2.5 Resultant forces and moments due to thermal load

If the temperature is independent of z, the temperature change can be removed from within the integrals, and the thermal force and moment resultants can be written as

$$N_x^T = \sum_{k=1}^{N} (Q_{11_k}\alpha_{x_k} + Q_{12_k}\alpha_{y_k} + Q_{16_k}\alpha_{xy_k})(z_k - z_{k-1})$$

$$N_y^T = \sum_{k=1}^{N} (Q_{12_k}\alpha_{x_k} + Q_{22_k}\alpha_{y_k} + Q_{26_k}\alpha_{xy_k})(z_k - z_{k-1})$$

$$N_{xy}^T = \sum_{k=1}^{N} (Q_{16_k}\alpha_{x_k} + Q_{26_k}\alpha_{y_k} + Q_{66_k}\alpha_{xy_k})(z_k - z_{k-1})$$

$$M_x^T = \frac{1}{2}\sum_{k=1}^{N} (Q_{11_k}\alpha_{x_k} + Q_{12_k}\alpha_{y_k} + Q_{16_k}\alpha_{xy_k})({z_k}^2 - {z_{k-1}}^2)$$

$$M_y^T = \frac{1}{2}\sum_{k=1}^{N} (Q_{12_k}\alpha_{x_k} + Q_{22_k}\alpha_{y_k} + Q_{26_k}\alpha_{xy_k})({z_k}^2 - {z_{k-1}}^2)$$

$$M_{xy}^T = \frac{1}{2}\sum_{k=1}^{N} (Q_{16_k}\alpha_{x_k} + Q_{26_k}\alpha_{y_k} + Q_{66_k}\alpha_{xy_k})({z_k}^2 - {z_{k-1}}^2)$$

Eq. 4.6

4.2.6 Overall CTE for the laminate and total strain due to thermal load

The values of the unit thermal stress resultants for the [±30/0] s were given and substituting these values, as well as the values of A11, A12, and A22, into the expressions for the coefficients of thermal expansion results in;

$$\alpha_x = \frac{A_{22}N_x^T - A_{12}N_y^T}{A_{11}A_{22} - A_{12}^2} \;;\; \alpha_y = \frac{A_{11}N_y^T - A_{12}N_x^T}{A_{11}A_{22} - A_{12}^2}$$

Eq. 4.7

Results,

$$\alpha_x = -2.16x10^{-6}/°C$$

&

$$\alpha_y = 16.80x10^{-6}/°C$$

Total strain due to thermal load after the substitution of CTE in the strain formula;

$$\varepsilon_x = 324\ x\ 10^{-6}$$
$$\varepsilon_y = -2520\ x\ 10^{-6}$$

4.2.7 Residual stresses in the laminate due to thermal load

Calculation of the residual stresses is again based on the values of the reduced stiffness and the values of α_x, α_y, and α_{xy}. These residual stresses can be illustrated like this after the application of Hooks Law:

RESIDUAL STRESSES: (By applying Hook`s Law)

$$\{\sigma\} = \begin{Bmatrix} 53.4 \\ 14.64 \\ 0 \end{Bmatrix} MPa \qquad \text{(For 0° Layer)}$$

$$\{\sigma\} = \begin{Bmatrix} -55.2 \\ 21.1 \\ -10.84 \end{Bmatrix} MPa \qquad \text{(For 30° Layer)}$$

$$\{\sigma\} = \begin{Bmatrix} -55.2 \\ 21.1 \\ 10.84 \end{Bmatrix} MPa \qquad \text{(For -30° Layer)}$$

4.2.8 Thermal strain and change in height through the thickness

We computed the laminate coefficients of thermal deformation by using classical lamination theory, incorporating the free thermal strain effects into the stress-strain

relations, defining thermal force resultants, and properly interpreting the strain response of the laminate subjected to a temperature change. Nothing was said about the thickness expansion of the laminate, yet an isolated layer has a thermal expansion coefficient of α_3 in the thickness direction and changes thickness by the amount t when the temperature is changed an amount T. At first thought one may innocently assume that an entire laminate expands by an amount T. After all, the thickness direction of the laminate and the thickness direction of each individual layer coincide. However, nothing could be further from the truth. If such an assumption was made, then it would indicate that nothing had been learned about the interaction of layers when they are in a laminate. How does a laminate respond in the thickness direction when heated and cooled? Can we define a through-thickness expansion coefficient for the laminate? How does it depend on a 3? To answer these questions, it is necessary to return to the case where free thermal strain effects are included in the three-dimensional stress-strain relations.

$$\varepsilon_{3_k} = \alpha_{3_k}\Delta T + S_{13_k}\sigma_{1_k} + S_{23_k}\sigma_{2_k}$$

Eq. 4.8

Where,

$$S_{13} = -\frac{v_{13}}{E_1} \qquad \& \qquad S_{23} = -\frac{v_{23}}{E_2}$$

$$\alpha_3 = 2.43x10^{-5}/°C$$

As an example of a thermally induced thickness change, consider the [±30/0] s laminate subjected to the cool down from the processing temperature of -150°C. The stresses in each layer that result from the free thermal deformation of the laminate. With a layer being 150 x 10-6 m thick, the thickness change for each of these four layers is given by equation;

$$\Delta h = \varepsilon_3 * h_o \quad \Rightarrow\Rightarrow \quad h_k = h_o - \Delta h \quad \Rightarrow\Rightarrow \quad \begin{Bmatrix} h_1 \\ h_2 \\ h_3 \\ h_4 \\ h_5 \\ h_6 \end{Bmatrix} = \begin{Bmatrix} 1.4934E-04 \\ 2.9869E-04 \\ 4.4804E-04 \\ 5.9740E-04 \\ 7.4675E-04 \\ 8.9609E-04 \end{Bmatrix} \boldsymbol{m}$$

4.2.9 Validation of results through Abaqus Simulation

For 3 layered symmetrical [±30/0] s laminate -degree graphite/epoxy laminate shell 181 is used as element. By using shell element laminate can be easily modeled. Where each shell thickness in case 1 is 0.005 m, Model is created by taking square cross section of each side of 0.15 mm and meshing is done by element edge length of 0.5, meshing is done for entire laminate at a time, 3 lamina are stacked on one other to get single laminate, each lamina consisting of matrix and fiber elements.

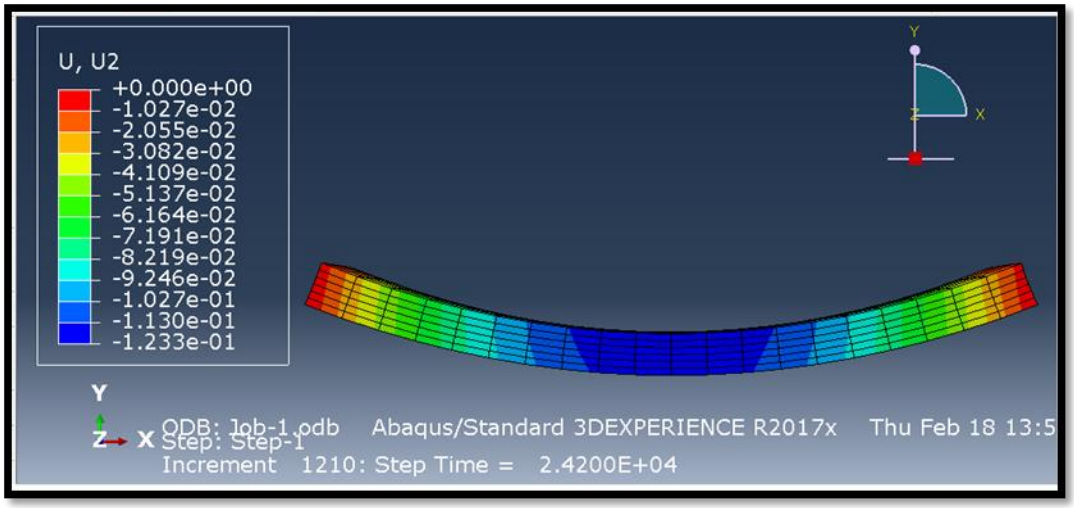

Fig. 4.8: Distortion due to thermal load in [±30/0] s laminate analyzed in Abaqus

4.2.10 Validation of results through CLT Software

In this case symmetric [±30/0] -degree graphite epoxy laminate is taken in to consideration and thermal loads are included under certain curing and room temperature along with mechanical loads. Fig. 4.9: [±30/0] s laminate -degree graphite epoxy laminate with fiber orientation Layers are stacked on one other with green color of fiber indicates 0-degree ply, blue color indicates 90-degree ply. Since this cross-ply laminate having 3 layers, it is

symmetric about its middle surface. This is the reason why, there is no coupling between bending and extension. Layer 1 is outer layer and fibers are in x direction, layer 2 is inner layer and fibers are in y direction, due to symmetry layer 3 is similar to layer 1. Thickness of both outer layers is equal to 0.127mm, Thickness of inner layer is equal to 10 times, thickness of outer layer 1.27 mm, Total laminate thickness is equal to 1.524mm.

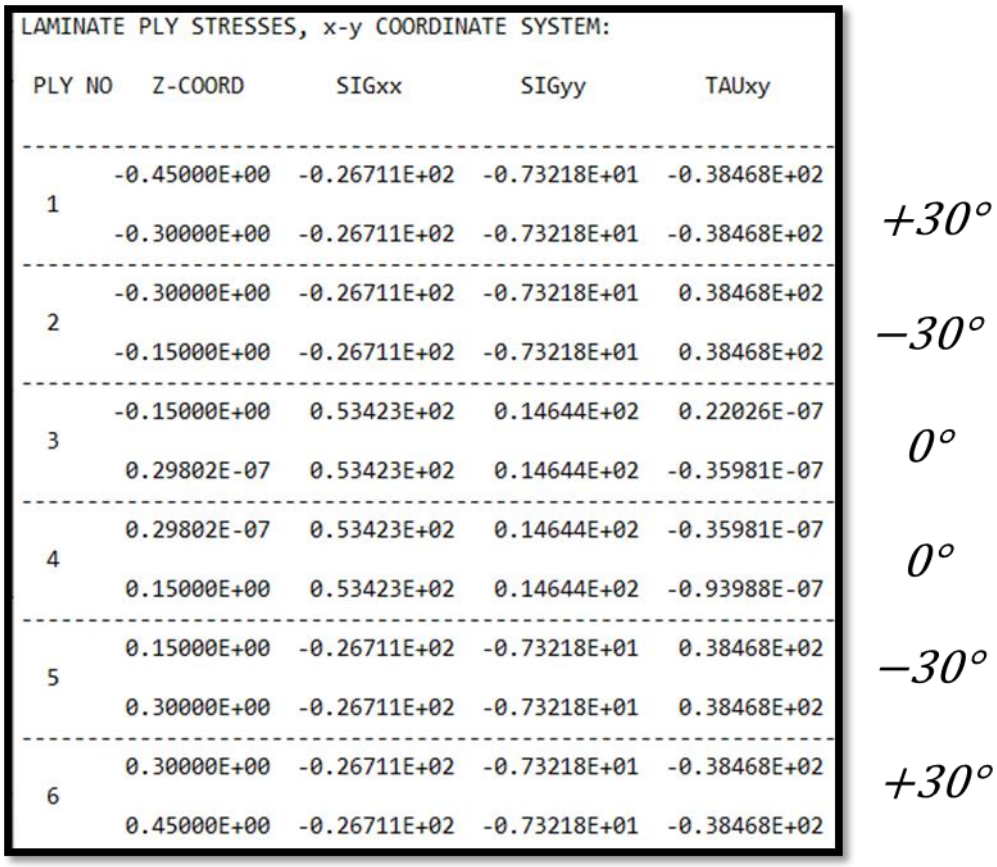

LAMINATE PLY STRESSES, x-y COORDINATE SYSTEM:

PLY NO	Z-COORD	SIGxx	SIGyy	TAUxy	
1	-0.45000E+00	-0.26711E+02	-0.73218E+01	-0.38468E+02	+30°
	-0.30000E+00	-0.26711E+02	-0.73218E+01	-0.38468E+02	
2	-0.30000E+00	-0.26711E+02	-0.73218E+01	0.38468E+02	−30°
	-0.15000E+00	-0.26711E+02	-0.73218E+01	0.38468E+02	
3	-0.15000E+00	0.53423E+02	0.14644E+02	0.22026E-07	0°
	0.29802E-07	0.53423E+02	0.14644E+02	-0.35981E-07	
4	0.29802E-07	0.53423E+02	0.14644E+02	-0.35981E-07	0°
	0.15000E+00	0.53423E+02	0.14644E+02	-0.93988E-07	
5	0.15000E+00	-0.26711E+02	-0.73218E+01	0.38468E+02	−30°
	0.30000E+00	-0.26711E+02	-0.73218E+01	0.38468E+02	
6	0.30000E+00	-0.26711E+02	-0.73218E+01	-0.38468E+02	+30°
	0.45000E+00	-0.26711E+02	-0.73218E+01	-0.38468E+02	

Fig. 4.9: Residual stress due to thermal load in [±30/0] s laminate analyzed in CLT program

4.3 Process Modelling with Thermoplastics

Thermoplastic polymers differ from their thermoset counterpart primarily by their melt temperature being lower than their decomposition temperature, while thermoset polymers have melting temperatures higher than their decomposition temperature, meaning that they cannot be reshaped upon melting. In molecular terms, this characteristic can be correlated to molecular weight, since an increase in molecular weight increases the

melting temperature. Thermoset have very high molecular weights because of the cross-links between their polymer chains, while thermoplastics have lower molecular weight since they are generally not cross-linked. This fundamental difference in physical properties between thermosets and thermoplastics has governed the development of their respective manufacturing techniques over the years with thermoplastic usually being melt processed while thermosets are exclusively reactively processed.

4.3.1 Materials

Elium®150 resin supplied from Arkema was used in this work. As an initiator, 2% Perkadox CH-50X Peroxide was mixed with the Elium® resin as recommended by the resin manufacturer [54]. A unidirectional (UD) glass fabric with an areal weight of 750 gsm (consisting of 660 gsm roving and 90 gsm random filament stitching) was used as the rein- forcing fabric

4.3.2 Polymerization kinetics model

To develop a polymerization kinetics model, isothermal and dynamic DSC experiments were carried out. The isothermal experiments were performed at three different temperatures 30 °C, 50 °C and 70 °C. It should be noted that it is a difficult task to reach a fully polymerized state after the isothermal polymerization at lower temperatures [55]. Therefore, dynamic DSC scans were also performed to obtain a complete polymerization and determine the corresponding total heat generation during the polymerization process. The dynamic DSC scans were carried out at three different heating rates of 5 ◦C/min, 7.5 ◦C/min and 10 ◦C/min. Nitrogen was used as a purge gas in the DSC experiments to prevent possible reaction inhibitions and oxidation of the polymer. From DSC experiments, heat flow vs. time and heat flow vs. temperature curves were obtained using the STAR e thermal analysis soft- ware. The total heat of reaction (ΔH tot) was calculated by integrating the heat flow with respect to time from the dynamic DSC tests. The final DoP (α) was calculated as:

$$\alpha = \frac{\Delta H}{\Delta H_{tot}} \; ; \qquad Eq.4.9$$

where ΔH was the heat generated by the reaction per unit mass of the resin at the end of the isothermal DSC tests. The resin was considered to be fully polymerized at α = 1 where α was the DoP. The rate of DoP, i.e. dα/dt, was assumed to be proportional to the rate of heat flow d(ΔH)/dt which is expressed as:

$$\frac{d\alpha}{dt} = \frac{d(\Delta H)}{dt} \chi \frac{1}{\Delta H_{tot}} \; ; \qquad Eq.4.10$$

Different polymerization kinetics models have been proposed and analyzed to describe the polymerization of the PMMA thermoplastic resin systems [56,57]. A well-known semi-empirical Arrhenius type autocatalytic model was used in this work for the rate of DoP as:

$$\frac{d\alpha}{dt} = A_1 \, exp\left(\frac{-E_1}{RT}\right)(1-\alpha)^{n_1} + A_2 \, exp\left(\frac{-E_2}{RT}\right)\alpha^{n_2}(\alpha_{max}-\alpha)^{n_3} \; ; \qquad Eq.4.11$$

where the reaction rate dα/dt was defined as a function of the DoP (α) and the absolute temperature T, with seven polymerization kinetic parameters namely the re-exponential constant Ai (i = 1,2), the activation energy Ei (i =1,2), the order of reaction kinetic exponents ni (i = 1,2,3) and the universal gas constant R, which was equal to 8.314 J/(mol·K). In Eq. 3, αmax was the maximum DoP that can be achieved at a certain isothermal temperature. Based on the obtained measured DoP rate from Eq. (1) and Eq. (2), the parameters in Eq. (3) were obtained by using the least squares nonlinear regression analysis in Matlab.

4.3.3 Heat transfer model

The general governing equation for the heat transfer problem was derived from the Fourier's heat conduction equation [58]:

$$\rho \, c_p \frac{\partial T}{\partial t} = \; k_x \left(\frac{\partial^2 T}{\partial x^2}\right) + \; k_y \left(\frac{\partial^2 T}{\partial y^2}\right) + \; k_z \left(\frac{\partial^2 T}{\partial z^2}\right) + Q^m \; ; \qquad Eq.4.12$$

where T is the temperature, t is the time and x, y, z are spatial co-ordinates in the Cartesian coordinate system, ρ, Cp and ki are the composite material's density, specific heat and thermal conductivity, respectively. The volumetric heat source term (Q^m) represents the

internal volumetric heat generation taking place during the polymerization of the resin and is expressed as,

$$Q^m = \rho\, \Delta H_{tot}\left(1 - V_f\right)\frac{d\alpha}{dt}\ ; \qquad Eq.4.13$$

where ΔH tot was the total reaction enthalpy during polymerization, Vf was the fiber volume fraction, dα/dt was the rate of polymerization re- action which was a function of DoP (α) and temperature (T) as shown in Eq. (3).

4.3.4 Boundary conditions & geometry

A three dimensional (3D) finite element (FE) model of the wind turbine blade was built to simulate the polymerization process of all the major components with in the blade. The developed process model was used to validate the polymerization kinetics model. blade cross section geometry was based on technical drawings of a wind turbine blade provided by a blade manufacturer.

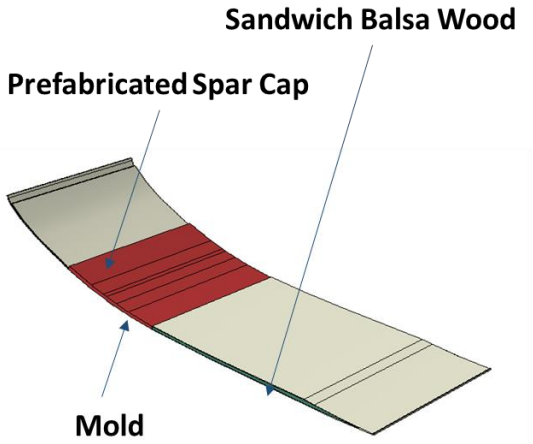

Fig. 4.10: Model of an outer shell with having all measure components

The transient heat conduction equation is coupled with the resin polymerization kinetics model given in Eq.4.13. The numerical process model was developed by using a general purpose FE software package ABAQUS to simulate the polymerization of the Elium® resin in the thermoplastic composite material. The nonlinear transient heat transfer solver in Abaqus/ Standard was used to simulate heat transfer.

In order to estimate the temperature and DoP evolutions during the vacuum infusion of wind turbine blade outer shell, a 3D model was developed in ABAQUS. Any free edges were assumed to be thermally insulated.

Inherent error and blade manufacturing processes are subject to the precision of manual labor and therefore variation. In order to reliably predict temperature and degree of polymerization in the Elium® resin, a parametric study on the material properties of the Elium® resin system as well as the glass fiber composite was conducted to show which parameters have the largest effect on the polymerization and therefore must be characterized more precisely.

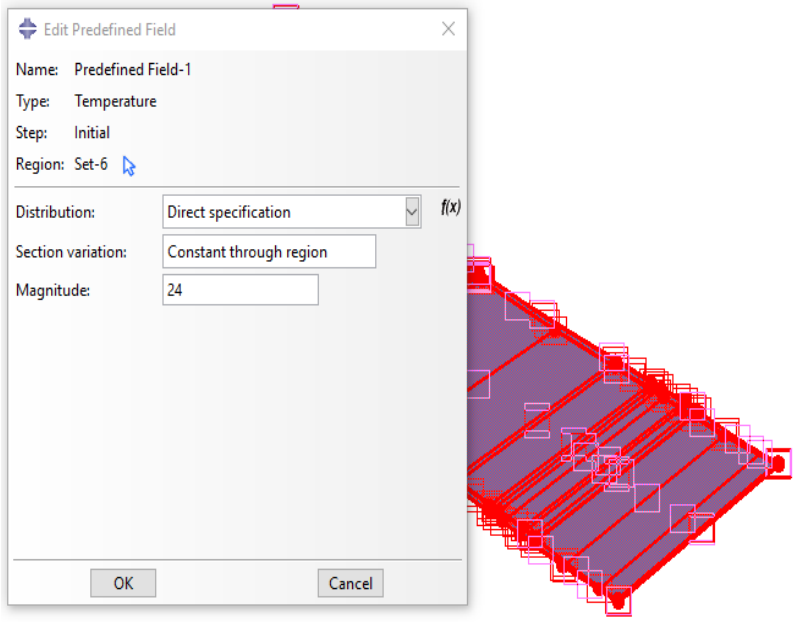

Fig. 4.11: Initial applied boundary condition

A script was created to vary each parameter ±25% from the baseline values, run the heat transfer model and track the development of temperature and degree of cure over time. Specifically, the results of interest are the adhesive peak temperature (Tpeak), the time until the peak temperature is reached (tpeak) and the time until the desired degree of polymerization is reached. A multiple linear regression was performed to analyze and estimate the influence of each material property on each output value.

The properties of the Elium® resin used in the FE model are shown in Table 4.1. The density of Elium® was obtained from the density measurement experiments. The heat capacity was obtained from the DSC experiments. The thermal conductivity was taken from [60]. For the sake of simplicity in the numerical simulations, the thermal properties of the Elium® resin were assumed to be constant as aforementioned which was also the case in [61] for PMMA since the changes in the thermal properties were described as relatively small during the polymerization. The thermal conductivity of Elium® composites was obtained by the rule of mixture [62].

Material properties of pure Elium® used in the thermo-chemical simulation of the polymerization in the water bath.

Material	ρ[kg/m^3]	C_p[J/kg·K]	k [W/m·K]
Elium®	1183 (measured)	1550 (measured)	0.18 [60]

Table 4.1: Properties of the Elium® resin

Here the thermal conductivity of the glass fiber was used as 0.18 W/(m·K) [59]. The employed PROPS of the laminates and the thermal properties used in the 3D thermal model are listed in Table 2.

PROPS#	PROPERTY	DESCRIPTION	VALUES	UNITS
1	A1	Pre-exponential Factor (1)	287140	sec-1
2	A2	Pre-exponential Factor (2)	1.9731	sec-1
3	Eα1	Activation Energy (1)	53711000	mJ/ mol-K
4	Eα2	Activation Energy (2)	7.49E+06	mJ/ mol-K
5	n1	Kinetic Constant	9.5308	-
6	n2	Kinetic Constant	1.4311	-
7	n3	Kinetic Constant	3.0202	-
8	H (tot)	Total Resin Reaction Enthalpy	2.41E+11	mJ/ tonne
9	R	Universal Gas Constant	8314	mJ/ mol-K
10	k, l	Thermal Conductivity (long.), Comp.	0.8	mW/ mm-K
11	k, t	Thermal Conductivity (trans.), Comp.	0.34	mW/ mm-K
12	k, t	Thermal Conductivity (trans.), Comp.	0.34	mW/ mm-K
13	cp, c	Specific Heat Capacity, Comp.	1.20E+09	mJ/ tonne-K
14	ρ , c	Density, Comp.	1.91E-09	tonne/ mm3
15	ρ , m	Density, Matrix	1.18E-09	tonne / mm3
16	v, f	Fiber Volume Fraction	0.55	-

Table 4.2: Homogenized material properties used for composite laminate having Elium® resin

Fig. 4.12 shows the mesh adopted in the model, which had the same element size across the cross section of the model. An 8-node linear brick elements (DC3D8) were used in the numerical model. The total number of elements was 204,800 for the complete outer shell model. The applied boundary conditions (BCs) in the model are shown in Fig. 4.12 & Fig. 4.13. The ambient temperature (T_{amb}) was set to 24 ◦C. The heat transfer coefficient of the laminate top surface (h_t) was assumed to be 5 W/(m2·K) interacted with the ambient temperature. It is worth noting that instead of modeling the glass mold, a convective heat transfer was defined at the bottom surface with a higher convective heat transfer coefficient (h_{bs}) [63].

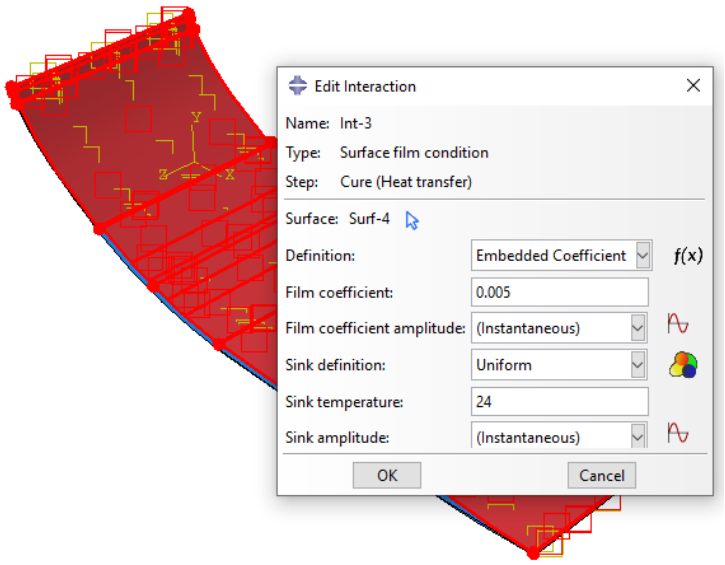

Fig. 4.12: Applied boundary condition at the top surface during the polymerization cycle

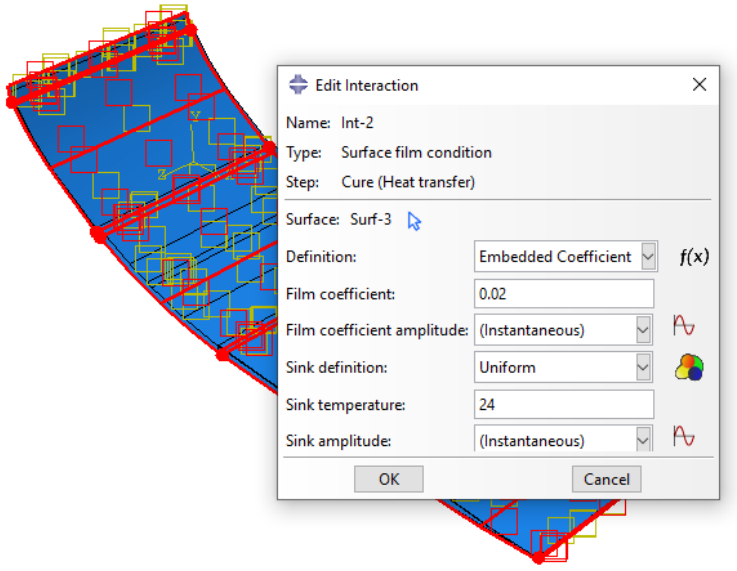

Fig. 4.13: Applied boundary condition at the bottom surface during the polymerization cycle

Two subroutines were implemented in ABAQUS to couple the general heat transfer equation with the polymerization kinetics model. In the subroutine USDFLD, DoP was calculated by using a Fortran code by employing the following relation in the time domain:

$$\alpha^{n+1} = \alpha^{n} + \left(\frac{\partial \alpha^{n}}{\partial t}\right) \Delta t \; ; n = 1,2,3,4 \ldots . \qquad Eq.4.12$$

where α^{n+1} was the DoP at the actual time step and αn represented the DoP at the previous time step. The variable α had to be initialized, and the value of 0.0001 was set as the initial DoP. The second subroutine HETVAL was employed to calculate the internal heat generation due the exothermic reaction. The FE software solves the coupled equations and outputs the temperature and DoP, allowing one to trace the thermal and polymerization histories during polymerization of the Elium® resin.

4.4 Results and Discussion

Under this heading, the results obtained from the process modeling of thermoplastic composites will be discussed. These results include temperature distribution and degree of polymerization during the manufacturing of outer shell. Necessary figures and graphs will be presented, while complete sets of profiles can be viewed at the end. The mesh was

confirmed to provide a converged solution. Spar cap material is fully cured and prefabricated while balsa wood is sandwiched between the composite laminate. Sections and materials were assumed to be perfectly connected thermally so that heat flux between different areas of the model was conducted without loss of thermal energy.

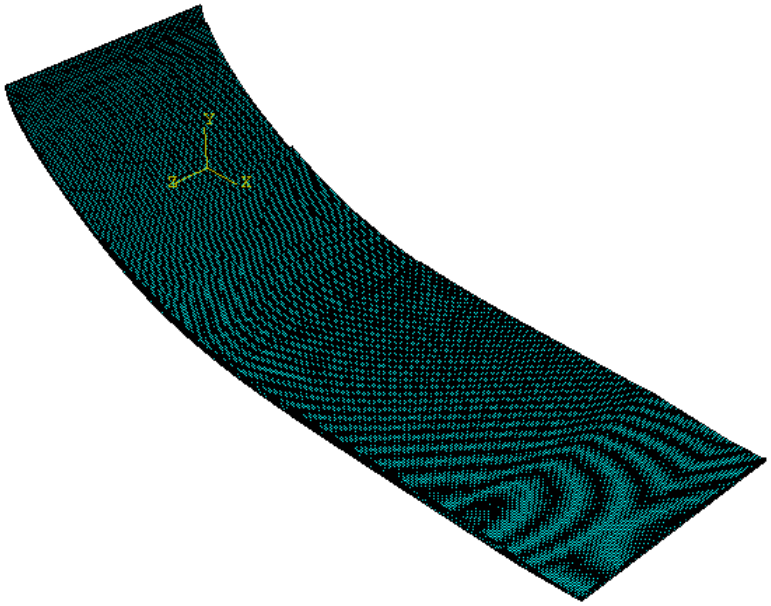

Fig. 4.14: Meshed outer shell model

In order to analyze the polymerization process, various points across the cross of the outer shell model has been chosen.

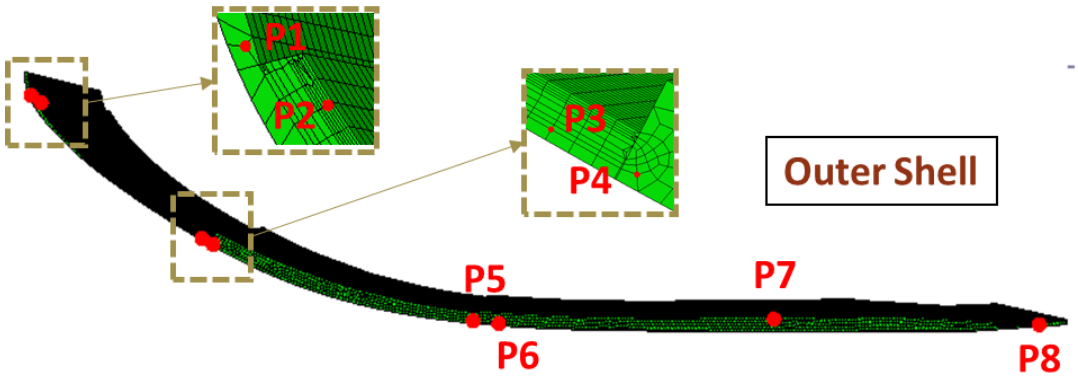

Fig. 4.15: Various points across the cross section of wind blade to analyze the polymerization process

Depicts the measured and predicted temperature evolution at the thermocouple location. It is seen that the thermal process model captured the main trends of the computationally observed internal heat generation quite well. The different peak temperatures were found across the various points of outer shell cross section. A total of 8 points were selected at the center of the resin to investigate the temperature evolution. The predicted peak temperatures and the corresponding process time matched quite well with the measured ones. It is seen that the regions with higher temperatures were located near the top surface because the heat was transferred in a faster way at the bottom and side surfaces than the top surface. Therefore, the heat was accumulated more near the top surface. Fig. 4.16 and Fig. 4.18 show the temperature and DoP histories of Elium® resin at different location points indicated in Fig. 4.15. It is seen that the temperature and DoP difference in the through-thickness direction increased with the increase in outer shell model temperature. In other words, an increase in the applied thermal load resulted in a more non- uniform polymerization reaction. The largest temperature difference was approximately 65 ◦C and 55 ◦C among the point 2 and 6. Overall, a good agreement was found between the measured and predicted temperature evolutions.

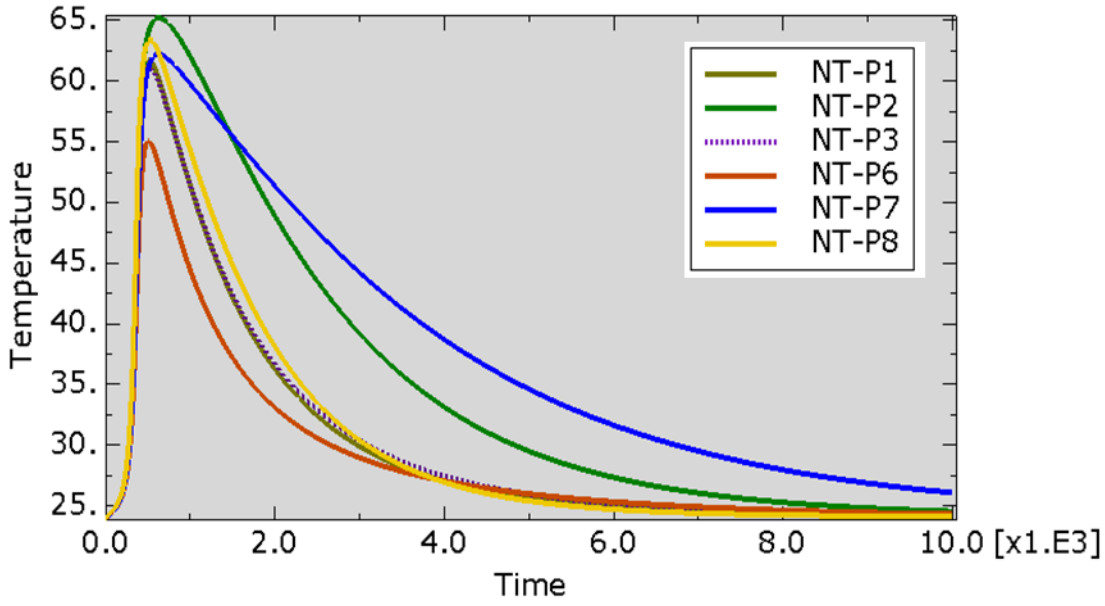

Fig. 4.16: Temperature distribution across the outer shell during the polymerization cycle

There are two evaluation points in the spar cap which also experience the change in temperature due to temperature variation nearby with the composite laminate.

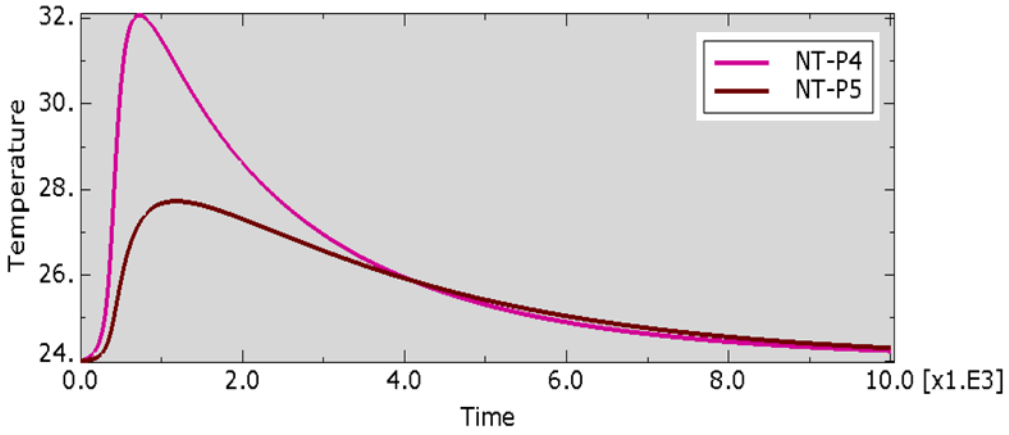

Fig. 4.17: Change in Temperature at the edges of spar cap during the polymerization cycle

Fig. 4.18 shows the plots of the predicted DoP across the various points of outer shell cross section (i.e., fully polymerized) for all the different composite laminate temperatures. The polymerization time is approximately in between 1500s and 2000s for all the different temperatures, respectively. The final DoP is reaching 1 due to the highly exothermal reaction of the Elium®. The polymerization time was different according to the different locations within the composite laminate. The region of a relatively fast polymerization time was at the bottom and side surfaces because the heating of the resin initiated earlier at the surfaces in contact with the water. Due to a lower internal generation and polymerization reaction rate for the points near to the bottom surface of outer shell, a lower final DoP was obtained. The polymerization time of thick laminates were found to be approximately above 500s for all the points depending upon the location. In Fig. 4.19, it is shown the detailed view of the degree of polymerization for all the different points to have a better visualization and understanding of the progression in the final results. The cooling rate of simulation at the bottom was faster than its experimental result which might be due to the assumptions made in the process model for the boundary conditions and material properties. It is seen that the maximum degree of polymerization took place near the top region of the laminates, as also observed with the thermocouple measurements.

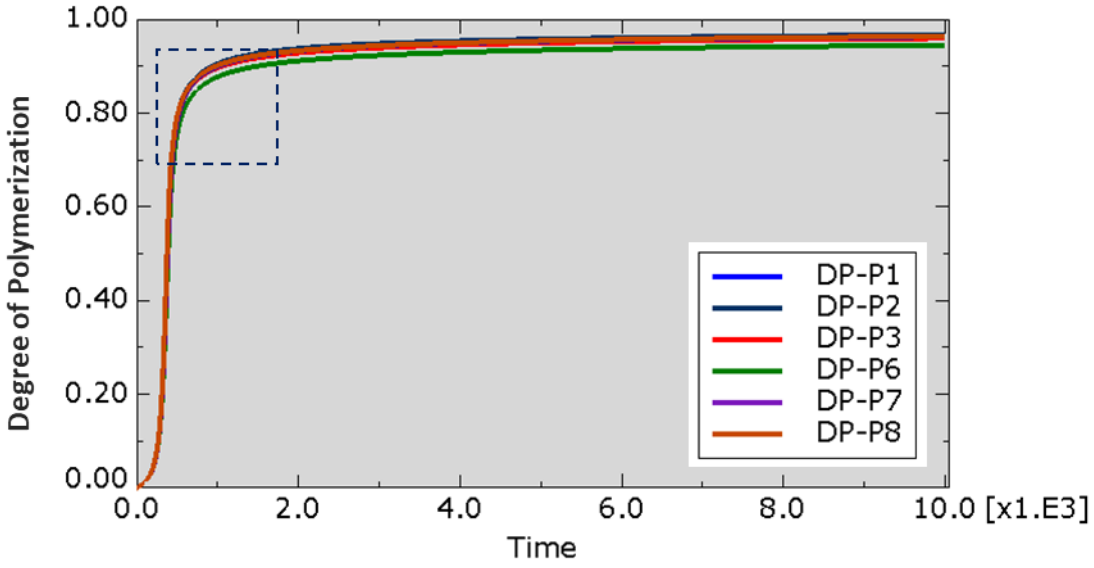

Fig. 4.18: Degree of polymerization across the outer shell during the polymerization cycle

The temperature difference in the thickness direction increased with an increase in laminate thickness, which also influenced the DoP, as seen in Fig. 4.19. Fig. 4.19 shows the DoP of different laminates at different points on the centerline along the thickness direction. The DoP was influenced by the temperature history of the laminate. The maximum DoP for all the points across the thickness of laminate was found to be around 0.92 and 0.97, respectively. This indicates that the maximum DoP increases with the increase of thickness of the laminate. This suggests that the DoP is different at different positions of laminate, and the highest difference of DoP increases with the increase of laminate thickness.

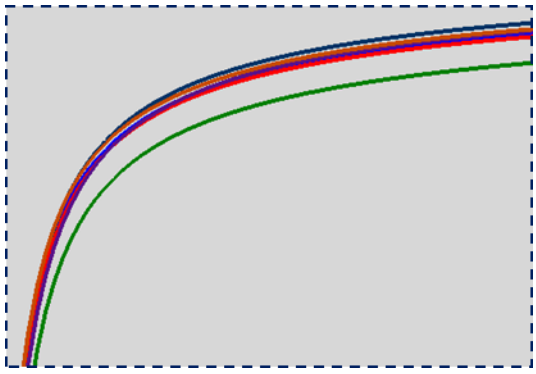

Fig. 4.19: Detailed view to analyze the degree of polymerization in outer shell

The reason could be the larger internal heat generation for the thicker laminates which results in a larger through thickness temperature and DoP difference. By using the developed numerical process model, the effect of laminate thickness and mold temperature (Room temperature (24 ◦C)) on the temperature peak was investigated as shown in Fig. 4.19. It is seen that the temperature peak increased with the laminate thickness and the mold temperature with a non-linear trend. The obtained temperature peaks were found to be lower than 100 ◦C. The change in temperature peak became less as the laminate thickness increased. In other words, the effect of thickness on the temperature peak was found to decrease for relatively thick laminates.

Chapter#5

5 Conclusion and recommendations

Computational characterization of polymerization overheating in thick glass/Elium® acrylic thermoplastic resin composites was studied with in model of wind turbine blade outer shell. First, the polymerization kinetics model of the pure Elium® resin was developed based on the DSC experiments. Subsequently, the polymerization kinetics model was coupled with the thermal model. The developed 3D thermo-chemical process model was validated with water bath experiments by taking the exothermic internal heat generation into account.

As a result, it was demonstrated that there is a need for qualitative and quantitative approaches to evaluating optimized polymerization cycles for the manufacturing of wind turbine blade outer shell that utilize composite materials. FE numerical models offer the ability to optimize cure cycles which ensure a rapid, uniform degree of polymerization throughout the manufacturing process and that do not exceed temperatures which will degrade the composite material, ensuring structural integrity in the long-term. Future experimental validation in lab conditions is proposed to validate the FE and to gauge the quality of the manufacturing process resulting from an optimized polymerization cycle. The effect of polymerization cycle parameters, such as convective coefficient and room temperature, as well as other unique geometries and conditions, are also to be explored in more depth.

A finite element model capable of predicting the composite temperature and polymerization over time in laminate was developed. Heat transfer equations were coupled with an analytical polymerization kinetics law. The polymerization kinetics model was characterized by non-isothermal DSC experiments and implemented using user subroutines. In the first part, a sensitivity study was performed to quantify the influence of each materials' thermal properties on the polymerization of the Elium® resin. Results showed that the polymerization behaviour is particularly sensitive to the specific heat Cp of the Elium® resin. In the second part, the polymerization kinetics were characterized, and the FE model was validated by comparison with experimental data of the temperature during polymerization of a thick composite laminate. Finally, a finite-element model of a blade cross-section was created and the temperature and

degree of polymerization of each different point across the outer shell cross section was investigated. The goal was to identify potential bottlenecks of the polymerization cycle and to virtually test improvement methods for shortening the cycle time. The results suggest that current manufacturing cycles are close to optimal for their existing setups. Critical aspects of the polymerization process have been identified and especially the polymerization of thin laminate and heat transfer through the spar cap area. Higher heating and cooling rates further accelerated the polymerization process. Delayed heat transfer through the thick spar cap area is a prominent challenge in blade manufacturing. In a realistic setting, manufacturers will have to decide which improvements and/or combinations are feasible and economical for their production cycle. This study demonstrates the potential of predictive tools in the design of wind turbine polymerization cycles.

Furthermore, the polymerization overheating was investigated by measuring the temperature evolution during the vacuum assisted resin infusion process for the manufacturing of wind turbine blade outer shell at room temperature. A 3D FE model of the composite laminate production across the various thicknesses was developed and investigated at different thermocouple measurements. It was found that the peak temperature increased from 55 ◦C to 65 ◦C as the laminate thickness increased from bottom to the top surface. A non-linear increase in peak temperature was obtained with an increase in laminate thickness and mould temperature. At last, the void content of Elium® composites was investigated and found to be lower than 1% for all the laminates. The proposed polymerization kinetics model, as well as the reported polymerization overheating trend can be used to further optimize the manufacturing processes of Elium® composites. More elaborate investigation of the effect of process temperature on the void formation for fibre reinforced Elium® composites is considered to be a future work.

5.1 Future Directions:

- For future work and in order to translate the results of this study into a realistic manufacturing context, adhesive temperature and degree of polymerization over time need to be verified experimentally during the bonding step in the production. Additionally, the results are highly sensitive to shape and thickness of the adhesive bond line during the second polymerization cycle for adhesive joining of all the different components together.

Therefore, ways to predict and confirm these dimensions need to be explored. Furthermore, prefabricated spar cap can be investigated computationally and then can be validated through experimental results.

- Future work also includes the enhancement of the model and coupling it with mechanical properties to study the effects of temperature and conversion gradients on the evolution of residual stresses within the bond line.

References

[1]. Van Rijswijk K, Bersee HE. Reactive processing of textile fiber-reinforced thermoplastic composites–An overview. Compos Appl Sci Manuf 2007;38(3): 666–81.

[2]. Yuksel O, Baran I, Ersoy N, Akkerman R. Investigation of transverse residual stresses in a thick pultruded composite using digital image correlation with hole drilling. Compos Struct 2019; 223:110954.

[3]. Baran I. Analysis of pultrusion process for thick glass/polyester composites: transverse shear stress formations. Adv Manuf Polym Compos Sci 2016:124–32.

[4]. Bogetti TA, Gillespie Jr JW. Process-induced stress and deformation in thick- section thermoset composite laminates. J Compos Mater 1992;26(5):626–60.

[5]. [5] Barbosa LC, Bortoluzzi DB, Ancelotti Jr AC. Analysis of fracture toughness in mode II and fractographic study of composites based on Elium® 150 thermoplastic matrix. Compos B Eng 2019; 175:107082.

[6]. Bhudolia SK, Gohel G, Fai LK, Barsotti Jr RJ. Investigation on ultrasonic welding attributes of novel carbon/elium® composites. Materials 2020;13(5):1117.

[7]. Bhudolia SK, Perrotey P, Joshi SC. Mode-I fracture toughness and fractographic investigation of carbon fibre composites with liquid methylmethacrylate thermoplastic matrix. Compos B Eng 2018; 134:246–53.

[8]. Zoller A, Escale P, Gerard P. Pultrusion of bendable continuous fibers reinforced composites with reactive acrylic thermoplastic ELIUM® resin. Frontiers in Materials 2019; 6:290.

[9]. Chilali A, Zouari W, Assarar M, et al. Analysis of the mechanical behaviour of flax and glass fabrics-reinforced thermoplastic and thermoset resins. J Reinforc Plast Compos 2016;35(16).

[10]. Bhudolia SK, Perrotey P, Joshi SC. Enhanced vibration damping and dynamic mechanical characteristics of composites with novel pseudo-thermoset matrixsystem. Compos Struct 2017; 179:502–13.

[11]. Boumbimba RM, Coulibaly M, Khabouchi A, et al. Glass fibres reinforced acrylic thermoplastic resin-based tri-block copolymers composites: low velocity impact response at various temperatures. Compos Struct 2016;160(1):939–51.

[12]. Kinvi-Dossou G, Matadi Boumbimba R, Bonfoh N, Garzon-Hernandez S, Garcia-Gonzalez D, Gerard P, et al. Innovative acrylic thermoplastic composites versus conventional composites: improving the impact performances. Compos Struct 2019; 217:1–13.

[13]. De A, Assarar M, Zouari W, et al. Effect of geometric dimensions and fibre orientation on 3D moisture diffusion in flax fibre reinforced thermoplastic and thermosetting composites. Compos Appl Sci Manuf 2017; 95:75–86.

[14]. De Andrade Raponi O, de Souza BR, Barbosa LCM. Thermal, rheological, and dielectric analyses of the polymerization reaction of a liquid thermoplastic resin for infusion manufacturing of composite Materials. A. C Polym Test 2018; 71:32–7.

[15]. Cadieu L, Kopp JB, Jumel J, Bega J, Froustey C. Strain rate effect on the mechanical properties of a glass fibre reinforced acrylic matrix laminate. An experimental approach. Compos Struct 2019; 223:110952.

[16]. Nash NH, Portela A, Bachour-Sirerol CI, Manolakis I, Comer AJ. Effect of environmental conditioning on the properties of thermosetting- and thermoplastic- matrix composite materials by resin infusion for marine applications. Compos B Eng 2019; 177:107271.

[17]. Kazemi ME, Shanmugam L, Lu D, Wang X, Wang B, Yang J. Mechanical properties and failure modes of hybrid fiber reinforced polymer composites with a novel liquid thermoplastic resin, Elium®. Compos Appl Sci Manuf 2019; 125:105523.

[18]. Pantelelis N, Bistekos E, Emmerich R, Gerard P, Zoller A, Gallardo RR. Compression RTM of reactive thermoplastic composites using microwaves and cure monitoring. Procedia CIRP 2020; 85:246–51.

[19]. Shin JH, Kim D, Centea T, Nutt SR. Thermoplastic prepreg with partially polymerized matrix: material and process development for efficient part manufacturing. Compos Appl Sci Manuf 2019; 119:154–64.

[20]. Murray RE, Penumadu D, Cousins D, Beach R, Snowberg D, Berry D, et al. Manufacturing and flexural characterization of infusion-reacted thermoplastic wind turbine blade subcomponents. Appl Compos Mater 2019;26(3):945–61.

[21]. Dylan S. Cousins a, *, Yasuhito Suzuki b, 1, Robynne E. Murray c, Joseph R. Samaniuk a,

Aaron P. Stebner. Recycling glass fiber thermoplastic composites from wind turbine blades. Journal of Cleaner Production, 2018;

[22]. Ning Hana,b, Ismet Baranb,**, Jamal Seyyed Monfared Zanjanib, Onur Yukselb, LuLing Ana,*, Remko Akkermanb. Experimental and computational analysis of the polymerization overheating in thick glass/Elium® acrylic thermoplastic resin composites. Composites Part B, 2020;

[23]. Kjelt VAN RIJSWIJK "THERMOPLASTIC COMPOSITE WIND TURBINE BLADES." VACUUM INFUSION TECHNOLOGY FOR ANIONIC POLYAMIDE-6 COMPOSITES Master thesis.

[24]. S.-S. Yao, et al. Recent advances in carbon-fiber-reinforced thermoplastic composites: A review Compos Part B: Eng, 142 (2018), pp. 241-250.

[25]. Y. Wang, et al. Compressive behavior of notched and unnotched carbon woven-ply PPS thermoplastic laminates at different temperatures. Compos Part B: Eng, 133 (2018), pp. 68-77

[26]. H.M. El-Dessouky, C.A. Lawrence. Ultra-lightweight carbon fibre/thermoplastic composite material using spread tow technology. Compos Part B: Eng, 50 (2013), pp. 91-97

[27]. C. Schneeberger, J.C.H. Wong, P. Ermanni. Hybrid bicomponent fibres for thermoplastic composite preforms. Compos Part A: Appl Sci Manuf, 103 (2017), pp. 69-73

[28]. S.K. Bhudolia, P. Perrotey, S.C. Joshi. Mode I fracture toughness and fractographic investigation of carbon fibre composites with liquid Methylmethacrylate thermoplastic matrix. Compos Part B: Eng, 134 (2018), pp. 246-253

[29]. A. Lystrup, T.L. Andersen. Autoclave consolidation of fibre composites with a high temperature thermoplastic matrix. J Mater Process Technol, 77 (1) (1998), pp. 80-85

[30]. R.T. Durai Prabhakaran. Are reactive thermoplastic polymers suitable for future wind turbine composite materials blades? Mech Adv Mater Struct, 21 (3) (2014), pp. 213-221

[31]. K. van Rijswijk, H.E.N. Bersee. Reactive processing of textile fiber-reinforced thermoplastic composites – An overview. Compos Part A: Appl Sci Manuf, 38 (3) (2007), pp. 666-681

[32]. Technical Datasheet "ELIUM® 150"

[33]. Derek Berry and David Snowbergf" Thermoplastic Composite Development for Wind Turbine Blades." Institute for advacnce composites manufacturing innovation.

[34]. Pooria Khalilia, Brina Blinzlera, Roland Kádára, Per Blomqvistb, Anna Sandingeb, Roeland Bisschopb, Xiaoling Liuc "RamiefabricElium® composites with flameretardantcoating: Flammability, smoke, viscoelastic and mechanical properties. Composites Part A.

[35]. K. Bhudolia 1,2, *, Pavel Perrotey 2 and Sunil C. Joshi 1,2 "" Optimizing Polymer Infusion Process for Thin Ply Textile Composites with Novel Matrix System". MDPI.

[36]. Olivia de Andrade Raponi1,2 | Lorena Cristina Miranda Barbosa1,2 | Bárbara Righetti de Souza1,2 | Antonio Carlos Ancelotti Junior1,2 "Study of the influence of initiator content in the polymerization reaction of a thermoplastic liquid resin for advanced composite manufacturing". Composites Part A.

[37]. Brøndsted P., Nijssen R., editors. *Advances in Wind Turbine Blade Design and Materials.* Woodhead Publishing; Oxford, UK: 2013. p. 484

[38]. Walker K. Renewable Energy Embraces Graphene: Improved Wind Turbine Technology.

[39]. Watson J.C., Serrano J.C. Composite Materials for Wind Blades. Wind Syst. Mag. 2010 :46–51.

[40]. Beckwith S.W. Resin Infusion Technology. SAMPE J. 2007; 43:66–70.

[41]. Mohamed M.H., Wetzel K.K. 3D Woven Carbon/Glass Hybrid Spar Cap for Wind Turbine Rotor Blade. Trans. ASME J. Sol. Energy Eng. 2006; 128:562–573. doi: 10.1115/1.2349543.

[42]. Joncas, S., van Rijswijk, K., Charron, J-F, Bersee, H.E.N., Beukers, A., Interfacial Shear Strength Properties of Vacuum-infused Anionic Polyamide-6 Glass-fiber

Composites. 47th AIAA/ASME/ASCE/AHS/ASC Structures, Structural Dynamics, and Materials Conference, Newport, Rhode Island, USA, 1-4 May 2006.

[43]. Van Rijswijk, K., Thermoplastic Composite Wind Turbine Blades – Vacuum Infusion Technology for Anionic Polyamide-6 Composites, PhD Thesis, Delft University of Technology, 2006.

[44]. Pillay, S., Vaidya, U.K., Janowski, G.M. Liquid Molding of Carbon Fabric-reinforced Nylon Matrix Composite Laminates, Journal of Thermoplastic Composites Materials, Vol. 18, November 2005.

[45]. Locke, J., Valencia, U., & Ishikawa, K. (2003, January). Design studies for twist-coupled wind turbine blades. In ASME 2003 Wind Energy Symposium (pp. 324-331). American Society of Mechanical Engineers.

[46]. Nijssen R.P.L. *Ph.D. Thesis.* Knowledge Centre Wind Turbine Materials and Constructions (KC-WMC); Wieringerwerf, The Netherlands: 2007. Fatigue Life Prediction and Strength Degradation of Wind Turbine Rotor Blade Composites.257p

[47]. Gasch, R.; Twele, J. Windkraftanlagen-Grundlagen, Entwurf, Planung und Betrieb; Springer: Berlin, Germany, 2011.

[48]. Wolters, C.; Lanaud, C. Rotor Blade Manufacturing and Testing. In Wissenschaft Triff Praxis— INNOVATIONEN für die Windenergie; Congress HUSUM Wind Energy: Husum, Germany, 2008.

[49]. Chen, X.; Zhao, X.; Xu, J. Revisiting the structural collapse of 52.3 m composite wind turbine blade in a full-scale bending test. Wind Energy 2017, 20, 1111–1127. [CrossRef]

[50]. Kleineberg, M. PräzisionsfertigungKomplexerCFK-ProfileamBeispielRumpfspant; German Aerospace Center: Braunschweig, Germany, 2008. (In German)

[51]. Klunker, F. Aspekte zur Modellierung und Simulation des Vaccum Assisted Resin Infusion; Papierflieger: Clausthal-Zellerfeld, Germany, 2008. (In German)

[52]. Nielsen, M.; Schmidt, J.W.; Hattesl, J.; Andersen, T.; Markussen, C. In situ measurement using FBGs of process-induced strains during curing of thick glass/epoxy laminate plate: Experimental results and numerical modelling. Wind Energy 2013, 16, 1241–1257.

[53]. Lahuerta, F.; Nijssen, R.P.L. Influence of Internal Temperature Development during Manufacturing on thick Laminates Compression Fatigue Properties. In IOP Conference Series: Materials Science and Engineering; IOP Publishing: Bristol, England, 2016.

[54]. Elium®150 Technical Datasheet. https://cstjmateriauxcomposites.files.wordpress.com.

[55]. Bernath, A., K¨arger, L., & Henning, F. Accurate cure modeling for isothermal processing of fast curing epoxy resins. Polymers. 2016; 8(11), 390.

[56]. Lee SN, Chiu MT, Lin HS. Kinetic model for the curing reaction of a tetraglycidyl diamino diphenyl methane/diaminodiphenyl sulfone (TGDDM/DDS) epoxy resin system. Polym Eng Sci 1992;32(15):1037–46.

[57]. Slesinger N, Fernlund G and Poursartip A. Development of a test method to validate cure kinetics models used in process simulation. In: SAMPE '10 spring symposium conference, Seattle, WA, 17–20 May 2010

[58]. Shi L. Heat transfer in the thick thermoset composites. Master. Thesis. Netherland: Delft University of Technology; 2016.

[59]. Shi L. Heat transfer in the thick thermoset composites. Master. Thesis. Netherland: Delft University of Technology; 2016.

[60]. Muthuraj Rajendran, Grohens Yves, Seantier Bastien. Mechanical and thermal insulation properties of Elium acrylic resin/cellulose nanofiber based composite aerogels. Nano-Structures & Nano-Objects 2017;12:68–76.

[61]. Suzuki Y, Cousins D, Wassgren J, et al. Kinetics and temperature evolution during the bulk polymerization of methyl methacrylate for vacuum-assisted resin transfer molding. Compos Appl Sci Manuf 2018;104:60–7.

[62]. Springer GS, Tsai SW. Thermal conductivities of unidirectional materials. Compos Mater 1967;1.

[63]. Nielsen MW. Predictions of process induced shape distortions and residual stresses in large fibre reinforced composite laminates. Ph. D. thesis. Lyngby, Denmark: Technical University of Denmark; 2012.

[64]. Akovali G, editor. Handbook of composite fabrication. iSmithers Rapra Publishing; 2001.